

NRC Publications Archive Archives des publications du CNRC

International Road Tunnel Fire Detection Research Project - Phase II Task 2: Full-Scale Fire Tests in a Laboratory Tunnel

Liu, Z. G.; Crampton, G. P.; Kashef, A.; Loughheed, G. D.; Gibbs, E.;
Muradori, S.

For the publisher's version, please access the DOI link below. / Pour consulter la version de l'éditeur, utilisez le lien DOI ci-dessous.

Publisher's version / Version de l'éditeur:

<https://doi.org/10.4224/20374374>

Research Report (National Research Council of Canada. Institute for Research in Construction), 2008-09-12

NRC Publications Archive Record / Notice des Archives des publications du CNRC :

<https://nrc-publications.canada.ca/eng/view/object/?id=33aeb027-a5cd-436d-b8a5-290c7630d1ab>

<https://publications-cnrc.canada.ca/fra/voir/objet/?id=33aeb027-a5cd-436d-b8a5-290c7630d1ab>

Access and use of this website and the material on it are subject to the Terms and Conditions set forth at

<https://nrc-publications.canada.ca/eng/copyright>

READ THESE TERMS AND CONDITIONS CAREFULLY BEFORE USING THIS WEBSITE.

L'accès à ce site Web et l'utilisation de son contenu sont assujettis aux conditions présentées dans le site

<https://publications-cnrc.canada.ca/fra/droits>

LISEZ CES CONDITIONS ATTENTIVEMENT AVANT D'UTILISER CE SITE WEB.

Questions? Contact the NRC Publications Archive team at

PublicationsArchive-ArchivesPublications@nrc-cnrc.gc.ca. If you wish to email the authors directly, please see the first page of the publication for their contact information.

Vous avez des questions? Nous pouvons vous aider. Pour communiquer directement avec un auteur, consultez la première page de la revue dans laquelle son article a été publié afin de trouver ses coordonnées. Si vous n'arrivez pas à les repérer, communiquez avec nous à PublicationsArchive-ArchivesPublications@nrc-cnrc.gc.ca.



<http://irc.nrc-cnrc.gc.ca>

International Road Tunnel Fire Detection Research Project - Phase II Task 2: Full-Scale Fire Tests in a Laboratory Tunnel

RR-270

Liu, Z.G.; Crampton, G.P.; Kashef, A.;
Lougheed, G.D.; Gibbs, E.; Muradori, S.

Sept. 12, 2008

The material in this document is covered by the provisions of the Copyright Act, by Canadian laws, policies, regulations and international agreements. Such provisions serve to identify the information source and, in specific instances, to prohibit reproduction of materials without written permission. For more information visit <http://laws.justice.gc.ca/en/showtdm/cs/C-42>

Les renseignements dans ce document sont protégés par la Loi sur le droit d'auteur, par les lois, les politiques et les règlements du Canada et des accords internationaux. Ces dispositions permettent d'identifier la source de l'information et, dans certains cas, d'interdire la copie de documents sans permission écrite. Pour obtenir de plus amples renseignements : <http://lois.justice.gc.ca/fr/showtdm/cs/C-42>



National Research
Council Canada

Conseil national
de recherches Canada

Canada

International Road Tunnel Fire Detection Research Project – Phase II

Task 2: Full-Scale Fire Tests in a Laboratory Tunnel

Prepared by

Z. G. Liu, G. Crampton, A. Kashef, G. Loughheed, E. Gibbs and S. Muradori

**Fire Research Program
Institute for Research in Construction
National Research Council of Canada, Ottawa, Canada**

International Road Tunnel Fire Detection Research Project – Phase II

Project Technical Panel

Frank Gallo, Port Authority of New York and New Jersey
Harry Capers, New Jersey DOT
Jesus Rohena, Federal Highway Administration
Paul Patty, Underwriters Laboratories Inc.
Volker Wetzig, Versuchs Stollen Hagerbach AG
Art Bendelius, A & G Consultants
Bill Connell, Parsons Brinckerhoff
Margaret Simonson, Swedish National Testing and Research Institute
Gary English, Seattle Fire Department
Peter Johnson, ARUP Fire Risk & Security
Jim Lake, NFPA staff liaison

Principal Sponsors

Ministry of Transportation of British Columbia
Ministry of Transportation of Ontario
Ministry of Transportation of Quebec
The City of Edmonton, Transportation Department, Transit Projects Branch
axonX LLC
Siemens Building Technologies
Tyco Fire Products
VisionUSA
Sureland Industrial Fire Safety
United Technologies Research Corporation

Contributing Sponsors

National Research Council of Canada
Port Authority of New York and New Jersey
A & G Consultants
PB Foundation
Micropack, Inc.
J-Power Systems and Sumitomo Electric U.S.A., Inc.
Honeywell Inc.

ABSTRACT

This report presents the research works completed in Task 2 of the International Road Tunnel Fire Detection Research Project – Phase II. The capabilities and limitations of nine fire detectors/detection systems were investigated in a laboratory research tunnel with various challenging fire scenarios.

The simulated tunnel fire scenarios used in the test program were pool fires located in the open space, underneath a vehicle and behind a large vehicle, stationary vehicle fires in the engine and passenger compartments as well as moving fires with two different speeds and driving directions facing the detectors. The fuel types included gasoline, propane, wood crib and plastic foam. Their fire sizes were varied from approximately 125 kW to 3,400 kW. Some fires grew very quickly to reach their maximum heat release rates in less than 30 s, while other fires in the test series grew very slowly, and it took more than 8 minutes to reach their maximum heat release rate. The fire characteristics generated from these fire scenarios, such as their fire growth rates, heat flux, temperature development and smoke spread in the tunnel, as well as their impacts on detecting performance were investigated.

The fire detectors/detection systems were selected from five types of fire detection technologies. They were: two linear heat detection systems, one optical flame detector, three CCTV fire detectors, one smoke detection system and two spot heat detectors. All the detectors/detection systems were evaluated under the same fire conditions. Their detecting performances, including their response times, fire locating and monitoring capabilities, to various tunnel fire scenarios were studied. Test results showed that their detecting capability to a fire incident in the tunnel was determined by fuel type, fire size, location and growth rate as well as their detecting mechanisms.

ACKNOWLEDGEMENTS

The project is conducted under the auspices of the Fire Protection Research Foundation (FPRF). The authors would like to acknowledge the support of the Technical Panel, Sponsors as well as many NRCC staff to this project. A special acknowledgement is noted to Kathleen Almand of the FPRF for her contribution in organizing the project.

TABLE OF CONTENTS

1. Introduction	6
2. Test Tunnel	7
3. Selected Fire Detection Systems and Their Setups in Tests	9
4. Instrumentations.....	18
5. Test Procedure.....	21
6. Fire Tests and Results	21
6.1 Pool Fires	22
6.1.1 Open Pool Fire.....	22
6.1.2 Pool Fires underneath Vehicle.....	23
6.1.3 Pool Fires behind Large Vehicle.....	38
6.2 Stationary Vehicle Fires.....	46
6.2.1 Engine Compartment Fires.....	46
6.2.2 Passenger Compartment Fires.....	51
6.3 Moving Fires.....	58
7. Summary.....	62
References.....	66

1. INTRODUCTION

A number of technical issues related to the use of the current fire detection technologies for road tunnel protection were identified in Phase I of the International Road Tunnel Fire Detection Research Project [1]. These issues were that relatively few test programs on the study of detecting performance of tunnel fire detection technologies were conducted. These programs mainly focused on the performance of linear heat detection systems and optical flame detectors. Many existing and newly developed fire detection technologies, such as spot heat detectors, smoke detection systems and visual CCTV flame and smoke detectors, were not studied systematically. The performances of detectors in these programs were evaluated mostly with pool fires that had a constant heat release rate of up to 3 MW. Impact of other fire scenarios, such as stationary and moving vehicle fires, on the detecting performance was not investigated.

The present work aims to study these concerns on the use of current fire detection technologies for road tunnel protection. A series of fire tests were conducted in a laboratory tunnel facility. The performance of nine fire detectors/detection systems selected from five types of fire detection technologies were evaluated with a variety of simulated tunnel fire incidents. These fire detectors/detection systems were: two linear heat detection systems, one optical flame detector, three CCTV fire detectors, one smoke detection system and two spot heat detectors. They provided a good representative of current fire detection technologies for use in tunnel fire detection.

All the detectors/detection systems were evaluated under the same fire conditions. The simulated tunnel fire scenarios included not only pool fires that had a fast growing rate and constant heat release rate, but also stationary vehicle fires that had a slow growth rate as well as moving vehicle fires. The fire sizes in the test series were varied from 125 kW to 3,400 kW and fuel types were gasoline, propane, wood crib and plastic foam. These fire scenarios were considered representative of the majority of tunnel fire incidents, and selected in Task 1 of the project [2].

This report presents works carried out in Task 2 of the International Road Tunnel Fire Detection Research Project (Phase II). The information on the testing tunnel, fire scenarios, fire detection systems and testing instrumentation is described. The fire characteristics generated from various simulated tunnel fire incidents, such as their fire growth rates, heat flux emitted, temperature development and smoke spread in the tunnel, are presented. The detecting performances of evaluated fire detectors/detection systems to various simulated tunnel fire incidents, including their response times, fire locating and monitoring capabilities, are reported.

2. TEST TUNNEL

The full-scale fire tests were carried out in a new laboratory research tunnel that was located at the NRCC facility site. The tunnel facility is 37.5 m long, 10 m wide and 5.5 m high (113 ft long, 30 ft wide, and 16.5 ft high). It can be used for conducting tests that realistically simulate fires in roadway and mass-transit tunnels. The tunnel has two end doors, one large side door to nearby burn hall at west end of the tunnel, and two side louvers at east end of the tunnel. Its constructions are shown in Figures 2.1 and 2.2.

Two end doors of the tunnel were closed during tests. Two side louvers at the east end of the tunnel, however, were partially opened, allowing fires in the tunnel to fully combust with sufficient air supply. The opening of two side louvers was 1.5 m wide by 4.9 m high at the north side, and 2.75 m wide by 4.9 m high at the south side.

Smoke produced in the tunnel facility can be collected and exhausted through a fan system. For the present work, however, only natural ventilation with ambient conditions was maintained and the mechanical ventilation systems in the tunnel did not operate during the tests. The effects of ventilation on the performance of fire detection systems will be studied separately in another task of the project.

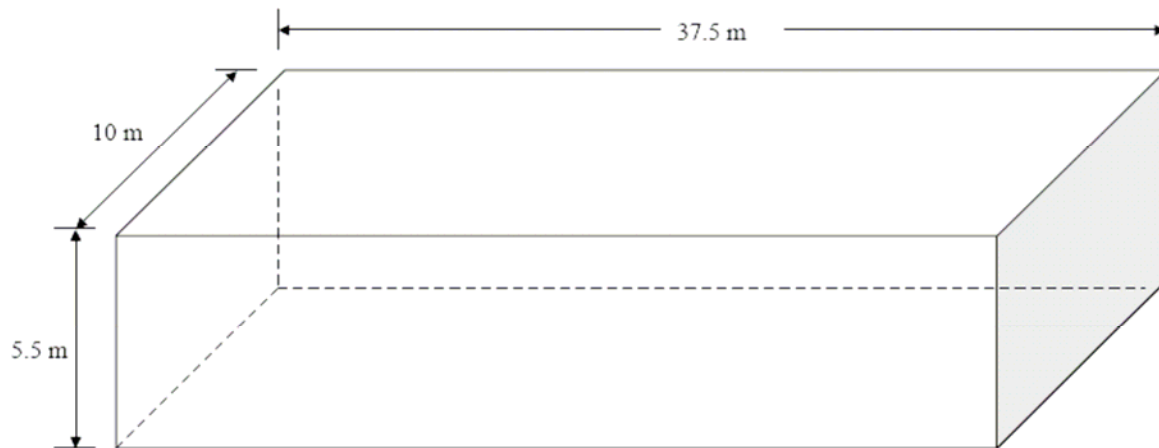


Figure 2.1. Schematic of the test tunnel



Figure 2.2. Overview of the test tunnel

3. SELECTED FIRE DETECTION SYSTEMS AND THEIR SETUPS IN TESTS

Nine fire detection systems were evaluated in the test program. These systems were selected by the Technical Panel from Task 1 of the project [2] and covered five types of currently available technologies. They were: two linear heat detection systems, one optical flame detector, three CCTV fire detectors, one smoke detection system and two spot heat detectors. General information on these systems is listed in Table 3.1 and their detecting mechanisms were described in the report of Task 1 [2].

Table 3.1. Fire Detection Systems in Test Program

Technology	System no.	System information	Alarming threshold	Detecting location
Linear heat	D-1L1	Fiber optic linear heat detection	Level 1: 50°C, 10°C/min; Level 2: 100°C, 15°C/min;	Two parallel cables in the tunnel, 2.5 m from the wall
	D-2L2	Analogue (co-axial cable) linear heat detection system	Alarming Temp: 70°C, Alarming rate: 7°C/min;	Two parallel cables in the tunnel, 2.5 m from the wall
Flame	D-3F1	IR3 flame detector	Sensitivity: 0.3 m x 0.3 m gasoline fire at 65 m on-axis and 45.7 m off-axis.	30 m from the fire source and 3.9 m from ground
CCTV	D-4C1	Visual flame and smoke detector	Flame: low (25); Offsite: 50% Smoke: normal	30 m from the fire source and 4.4 m from ground
	D-5C2	Visual flame detector	See Table 3.3	30 m from the fire source and 4.2 m from ground
	D-6C3	Visual flame detector	Sensitivity: 10 kW fire at 30 m.	30 m from the fire source and 3.8 m from ground
Spot heat	D-7H1	Heat detector with a fixed temperature	79.5°C fast response bulbs	3 m spacing at the center of tunnel ceiling
	D-8H2	Rate-anticipation heat detector	Alarming Temp: 57.2°C	15.2 m spacing at the center of tunnel ceiling
Smoke	D-9S1	Air sampling system	Fire threshold: 0.062%/ft	Air sampling line at the center of tunnel ceiling

It was required that the configuration and installation of fire detection systems in the test tunnel were designed for providing a protection for a road tunnel with a dimension of 10m wide x 5.5 m high x 2,000 m long (30 ft x 16.5 ft x 6,100 ft long) [2]. Their installation configurations were not allowed to change during tests. The sensitivity levels or alarming thresholds of fire detection systems were also not allowed to change during tests. They shall be the same ones as used in operating tunnels and be consistent with those used in the operating environment tests in the Lincoln tunnel undertaken in Tasks 5 and 6 of the project.

According to these requirements, all the selected fire detectors/detection systems were installed in the test tunnel by the system suppliers. The configurations of nine detectors/detection systems in the test tunnel are shown in Figure 3.1. They were evaluated under the same fire test conditions. The outputs of these detection systems were sent to a data acquisition system.

System D-1L1 was a fiber optic linear heat detection system based on Raman scattering. The entire optical fiber was used as the sensing medium. Fire warning signals could be given based on rate of temperature rise and/or exceeding a fixed temperature. During the test program, two levels of alarm threshold were set up. The alarming temperature and the rate of temperature rise were 50°C and 10°C/min for Level 1 of the threshold and 100°C and 15°C/min for Level 2 of the threshold. The fire location in the tunnel could be identified according to the temperature distribution along the fiber cable. The space resolution of the system for a fire location was 1.2 m.

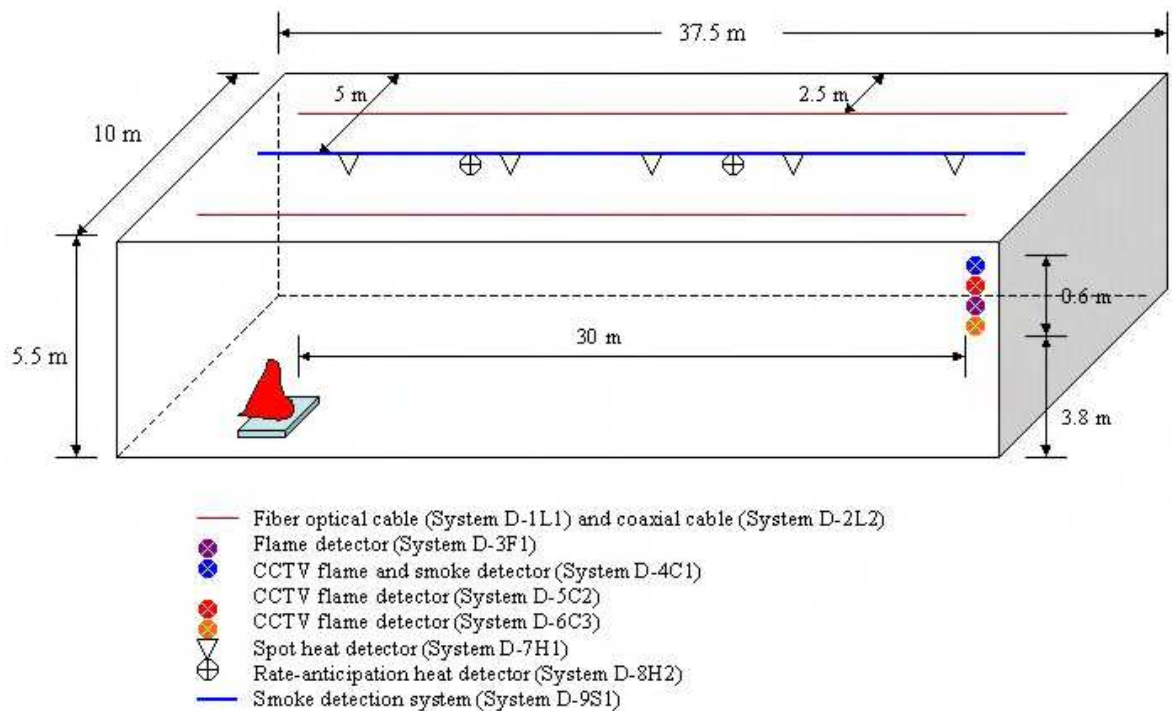


Figure 3.1. Schematic of detector setup in the test tunnel

Two parallel sensing cables of System D-1L1 were installed on the ceiling of the tunnel (see Figure 3.1). Each cable was located at approximately 80 mm from the ceiling, 2.5 m from the wall and 5 m from another sensing cable. A total 2,198 m length of the sensing cable was used in the test program. The cable section installed in the tunnel was from 2,000 m to 2,198 m, which is the maximum sensing length of the system recommended by the supplier. The fiber optic cable in the tunnel facility was protected with a 2 mm diameter's stainless tube. The detailed configuration of the sensing cable in the test program is shown in Figure 3.2.

System D-2L2 was an analogue (coaxial cable) linear heat detection system. The sensor cable consisted of a conductor, an insulating layer, and a metal-weaving screen layer. Fire warning signals could be given based on rate of temperature rise and/or exceeding a fixed temperature. During tests, the alarming temperature and the rate of temperature rise of the system were 70°C and 7°C/min.

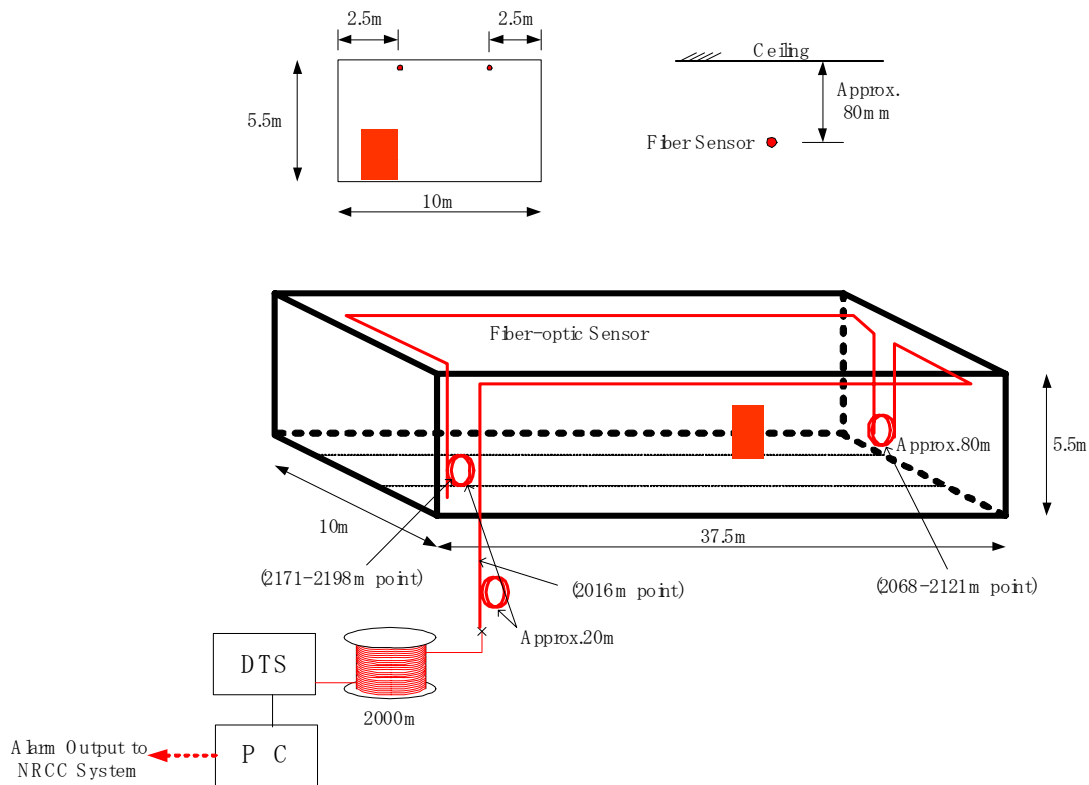


Figure 3.2. Configuration of System D-1L1 in the test tunnel

The configuration of the sensing cable of System D-2L2 in the test tunnel was similar to that with System D-1L1. 2 parallel sensing cables were installed on the ceiling of the tunnel (see Figure 3.1). Each cable was located at approximately 80 mm from the ceiling, 2.5 m from the wall and 5 m from another sensing cable. A total approximately 90 m long sensing cable, as one detecting section of the system, was installed in the test tunnel. Figure 3.3 is the picture showing sensing cables of both System D-1L1 and System D-2L2 below the ceiling of the tunnel.



Figure 3.3. Sensing cables of Systems D-1L1 D-2L2 on the ceiling of the tunnel

System D-3F1 was a multi-spectrum infrared (IR) flame detector. It consisted of three IR sensors: one covered the typical CO₂ flame emission spectral band that was responsible for the detection of flame radiation, and the other two sensors cover different, adjacent, and specially selected spectral bands, where black body emitters and background radiation were produced and they were used to minimize false alarms. The detector was installed at the north sidewall of the test tunnel, and at 3.9 m from the ground (see Figures 3.1 and 3.4). Its sensitivity was set to be “very high” for a 0.3 m x 0.3 m gasoline pool fire at 65 m on-axis and 45.7 m off-axis.

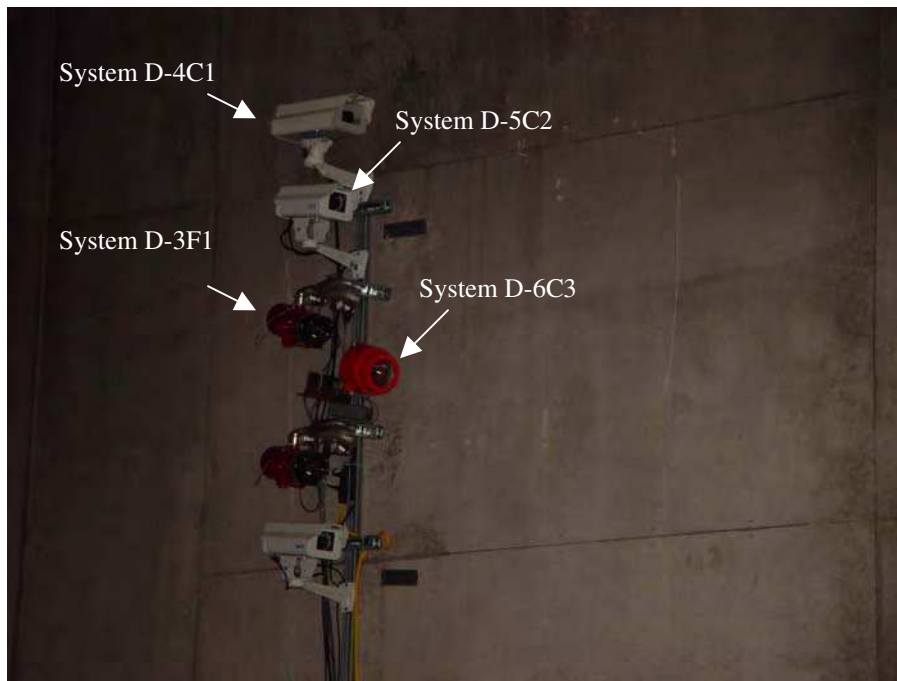


Figure 3.4. Configuration of flame and visual detectors in the test tunnel

System D-4C1 was a Closed Circuit Television (CCTV) flame and smoke detection system. Fire alarms were issued, once the characteristics of flame and smoke generated in a fire incident were identified. For the current test program, the detector was installed at the north sidewall of the test tunnel, and at 4.4 m from the ground (see Figures 3.1 and 3.4). The image of the system ran parallel with the wall of the tunnel. The entire tunnel was covered starting at 18.0 m from the camera, and the preceding camera would cover the blind spot of the camera in front of it. The view of the tunnel covered by the camera is shown in Figure 3.5. The detector had two flame algorithms and one smoke alarm algorithm. The first flame algorithm was used to detect the fire in the field of view of the camera and the second one “Offsite” was used to detect the fires outside the field of view. Its sensitivity settings during test program are listed in Table 3.2.

Table 3.2. Sensitivity settings in System D-4C1

Setting	FSM8
Flame	Low (25)
Offsite	50%
Smoke	Normal
Outdoor	Checked



Figure 3.5. Coving view of the test tunnel provided by System D-4C1

System D-5C2 was the second CCTV detection system. It detected a fire mainly based on the characteristics of the flame generated from a fire incident. During the test program, the detector was located at the north sidewall of the test tunnel, and at 4.2 m from the ground (see Figures 3.1 and 3.4). The detector was able to cover the entire tunnel. The view of the tunnel covered by the camera is shown in Figure 3.6. Its sensitivity settings during tests are listed in Table 3.3.

Table 3.3. Sensitivity settings in System D-5C2

Intensity	Mean Crossing	Intensity Standard Deviation	Flicker Mask Counter Bit Mask	Flicker Mask Counter	Color
64	4	16	127	16	yes



Figure 3.6. Coving view of the test tunnel provided by System D-5C2

System D-6C3 was the third CCTV detection system. It detected a fire also based on the characteristics of the flame generated in a fire incident. Unlike Systems D-4C1 and D-5C2, image sensing and processing of System D-6C3 were combined into one detector, and fire information and videos were directly sent to the monitoring computer through a controller, once a fire incident was identified. During the test program, one detector was located at the north sidewall of the test tunnel, and at 3.8 m from the ground (see Figures 3.1 and 3.4). No image of the test tunnel and experimental setup was demonstrated on the screen of the monitoring computer, and the flame image was demonstrated only after the fire was detected. The sensitivity of the detector during the test program was set to be a level for detecting a 10 kW fire at approximately 30 m.

System D-7H1 was a pneumatic, spot type heat detection system based on frangible bulb technology. The device was fitted on a sensing line pressurized using nitrogen. A fire signal was given when the frangible bulb was broken during a fire incident, and the air trapped in the line was released. During the test program, two 15 m long zones of 12.7 mm steel pipe were installed along the center of the test tunnel (see Figure 3.1). Five 79.5°C fast response sprinkler heads were installed per zone at 3 m spacing and at 20 cm from the ceiling. The overview of the system on the ceiling of the tunnel is shown in Figure 3.7. During testing, the pipe was pressurized with approximately 20 psi of compressed air, by way of a near-by compressor. The compressor was run continuously to make up for any small leaks that may have been existent in the installation.

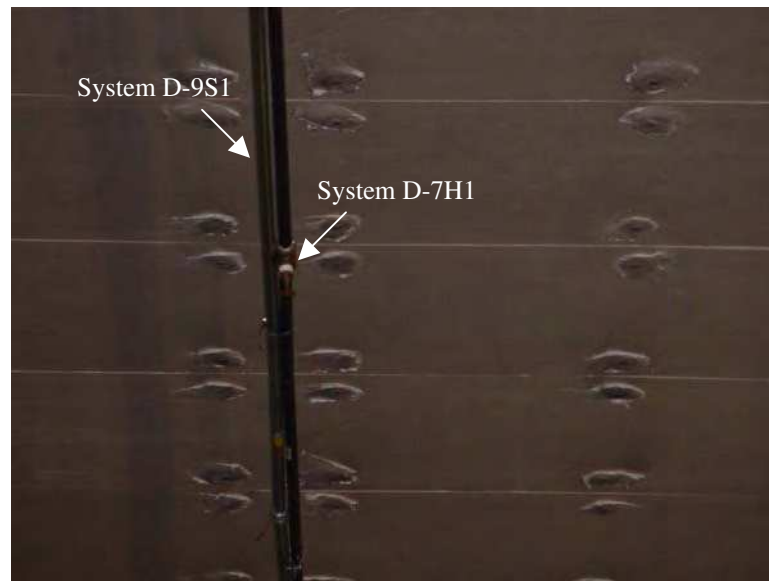


Figure 3.7. Overview of System D-7H1 and System D-9S1 in the test tunnel

System D-8H2 was a rate-anticipation spot heat detector. It responded and activated the fire alarm when the ambient temperature reached the preset temperature setting. Its protected area was 15.24 m x 15.24 m. For the current test program, two 57.2°C responded heat detectors were installed along the center of the tunnel ceiling (see Figure 3.1) at 15 m spacing and at 11 cm from the ceiling.

System D-9S1 was an air sampling-type smoke detection system. Air was continuously drawn into a pipe network through holes in the piping to a centrally-located smoke detector using an air pump or aspirator. Alarms were issued, if the amount of smoke in the sampled air exceeded the thresholds. For the current test program, a 34 m long sampling pipe with 6 sampling holes in 5.6 m spacing was installed along the center of the tunnel ceiling (see Figure 3.1). The pipe installed in the test tunnel represents 28% of the total coverage area of one smoke detector in a real tunnel as well as in the operating environment tests in the Lincoln tunnel undertaken in Tasks 5 and 6 of the project. In order to match the air flow sampled in a full coverage area of a smoked detector, 28% of the airflow through the detector was sampled through the pipe installed the test tunnel during tests. The overviews of the pipe in the test tunnel are shown in Figures 3.7 and 3.8.

A number of additional fire detectors, including spot heat detectors, flame and CCTV detectors, were also installed in the test tunnel for collecting extra test data (see Figures 3.4 and 3.8). These additional detectors were not connected to the project data collection system, but to the data collection systems of the system suppliers. Their performances are not presented in the report.

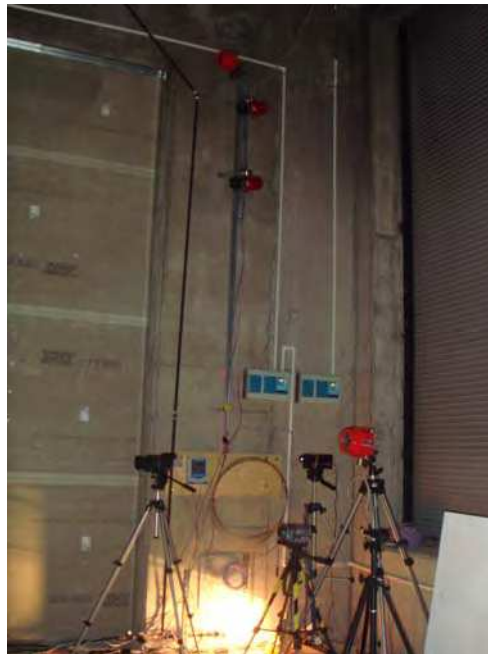


Figure 3.8. Overview of configuration of detectors on the south wall of the tunnel

4. INSTRUMENTATIONS

Various instruments were used to monitor fire tests. They included thermocouples, heat flux meters, smoke meters, velocity meters and video cameras, as shown in Figure 4.1. The locations of each instrument in the tunnel were shown in Figure 4.2.

Fifty-five thermocouples (Type K, 18 gauge, Figure 4.1f) were installed at the ceiling of the tunnel facility for temperature measurements. As shown in Figure 4.2, the transverse and longitudinal distances between thermocouples on the ceiling of the tunnel are 1.67 m and 3.125 m, respectively, and each thermocouple was at 15 cm from the ceiling. Two thermocouple trees were dropped from the ceiling of the tunnel. One was located above the fire to measure the gas/flame temperatures of the fire source and to monitor the fire development. The second one was located at the middle of the tunnel (18.7 m from the end of the tunnel and 5 m from the wall of the tunnel) to monitor fire development in the tunnel. There were five thermocouples on each tree: 0.5 m distance from the ground and to the ceiling, and 1.1 m interval distance between the thermocouples.

Three smoke meters were used for measuring smoke optical density in the tunnel (Figure 4.1d). They were located at the middle of the tunnel and approximately 12 m from the fire source. One sampling-obscurator smoke system was used to measure the smoke from the hot layer and its sampling port was located at 15 cm from the ceiling. Two straight-line obscuration smoke systems were used to measure the smoke density at low portion of the tunnel (1.53 m and 2.5 m from the ground). The measuring methods of these two types of smoke meters are described in a NRC research report [3].

Hand held Dwyer VT140 Thermo-anemometers with the remote vane sensors mounted on 4 m long aluminum poles were used to measure the air/gas velocity in the tunnel (Figure 4.1a). The measurements were taken at the middle of the tunnel from 3 heights: 15 cm from the ceiling, 2.75 m from the ground and 0.7 m from the ground.

Five heat flux meters and radiometers were used to measure the heat and radiant flux of the fire, and to monitor the fire development (Figure 4.1b). They were located, respectively, at 1 m, 2 m, 5 m, 10 m and 29 m from the fire source, and at 1.45 m from the ground, as shown in Figure 4.2. The radiometer that was located at 29 m from the fire source was placed near the end of the tunnel close to the flame detectors, which was used to measure flame radiant that could reach the detectors.

Two regular Sony Hi8 digital video cameras were used to provide a video record for the tests (Figure 4.1e). One video camera was located near the fire source to monitor the flame conditions around mock-ups. The second one was located at 29 m from the fire source to monitor the fire development in the tunnel.

The locations and distributions of these instrumentations remained unchanged in the test program. These test data together with outputs of the detection systems were collected at one second intervals by a data acquisition system (Figure 4.1c).



Figure 4.1a). Velocity meter

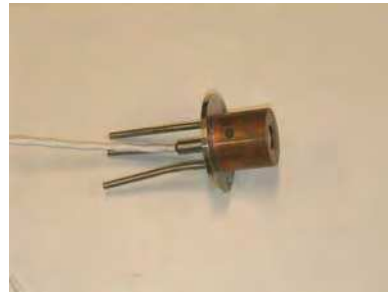


Figure 4.1b). Heat flux



Figure 4.1c). Data Collection system



Figure 4.1d). Smoke meters



Figure 4.1e). Video Camera



Figure 4.1f). Thermocouple

Figure 4.1. Some instrumentation in the test program

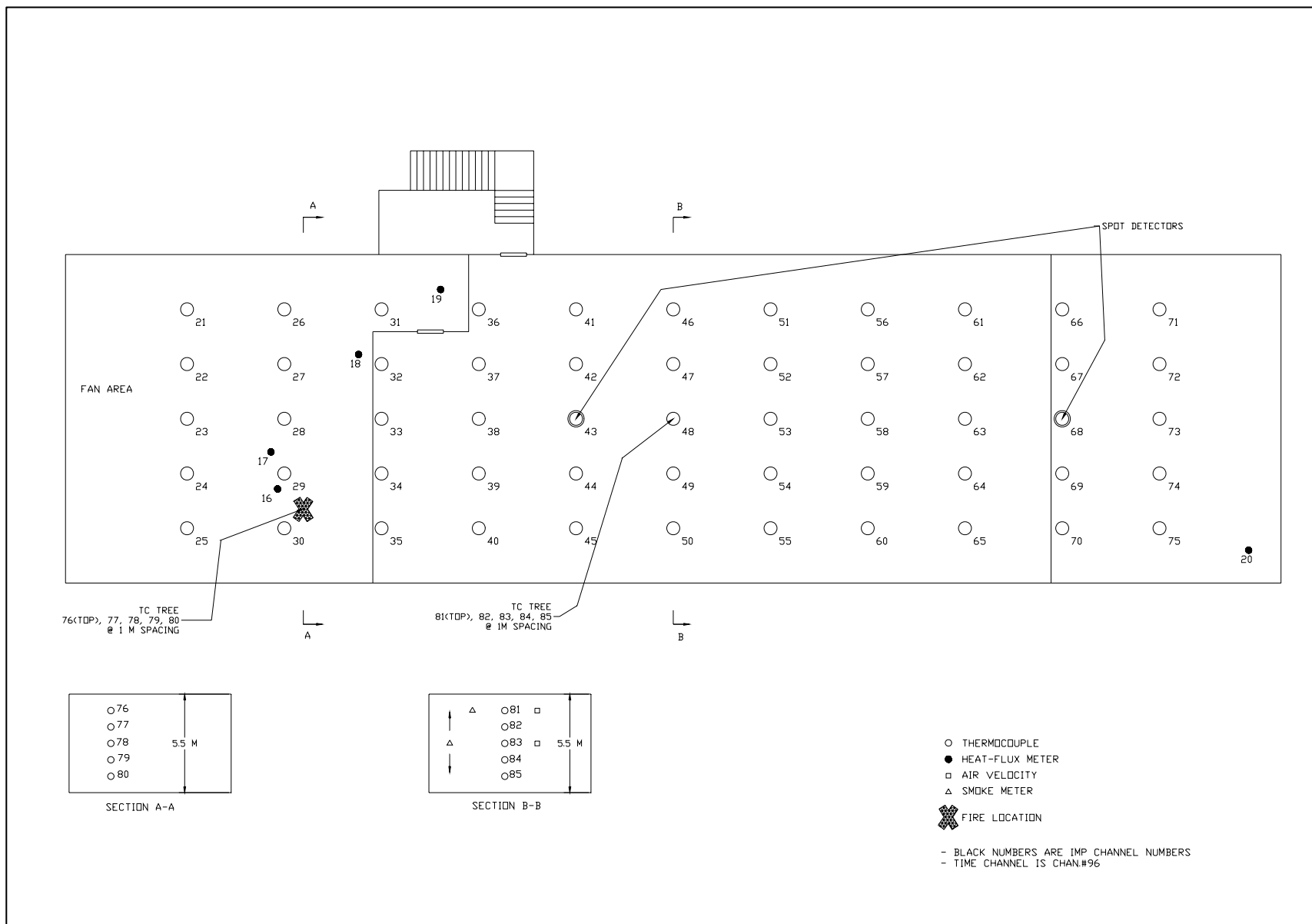


Figure 4.2. Schematic of instrumentation in the test tunnel

5. TEST PROCEDURE

The general test procedure in the test program was as follows:

- Prepare fire scenarios;
- Check instrumentation and each detection system prior to each test, to assure normal operation;
- Start the data acquisition system and video recorders for 60 s, and then manually ignite the fire;
- Terminate the test when:
 - All the detectors activate;
 - Or 4 minutes after the fire reaches its maximum heat release rate;
 - Or a maximum safe operating temperature at the ceiling is reached, which is defined to be 200°C ceiling temperature at 3 m from the fire source. This is designed to ensure that the detection systems mounted in the tunnel are not damaged.
- Check each detection system to determine if they still function properly after the fire test.

6. FIRE TESTS AND RESULTS

Twenty-one full-scale fire tests involving three types of tunnel fire scenarios were conducted in the test tunnel. These fire scenarios included gasoline pool fires in open space, underneath the vehicle and behind the vehicle, stationary vehicle fires in engine and passenger compartments and moving vehicle fires. The fire sizes varied from approximately 125 kW to 3,400 kW and fuel types included gasoline, propane, wood crib and plastic foam. These fire scenarios were considered representative of the majority of tunnel fire incidents, and selected in Task 1 of the project [2]. The fabrications of these fire setups were also prepared and reported in Task 1 of the project [2].

For the tests involving liquid pool fires and stationary passenger vehicle fires, the fire source was placed at the same location in the test tunnel: 6.5 m from east end of the tunnel and 2.5 m from north wall of the tunnel or at the side lane of the tunnel. For this position, the fire source was located below sensing cables of Systems D-1L1 and D-2L2; at 30 m from the optical flame and CCTV detectors (Systems D-3F1 to D-6C3); at approximately 3 m from a nearest sprinkler head of System D-7H1; at approximately 7.5 m from a nearest spot heat detector of System D-8H2; and at approximately 4 m from a nearest sampling hole of System D-9S1.

The fire characteristics generated from various fire scenarios, such as their fire growth rate, temperature distribution and smoke spread in the tunnel, were investigated. The detecting capability and limitation of the selected fire detectors/detection systems were evaluated under the same fire test conditions. The detecting time of each detector/detection system in the test series, which was defined as the interval between the fire ignition point and the alarm activating point of the system, was recorded. The locating and monitoring capabilities of some detection systems on a fire incident were also evaluated.

6.1. Pool Fires

Pool fire scenarios used in test series included an open gasoline pool fire, gasoline pool fires underneath a vehicle, and gasoline pool fires behind a large vehicle. A propane burner with a controlled heat release rate was also used for simulating pool fires underneath a vehicle. The test conditions and results, involving pool fire scenarios, are listed in Table 6.1.

6.1.1. Open Pool Fire

A gasoline pan with the size of 0.3 m x 0.3 m was placed at the north side lane of the test tunnel. There was no obstacle around the fire source. Ambient temperature in the tunnel was 6°C and there was no air velocity in the tunnel. The test was designed for evaluating performances of detectors/detection systems to a small open pool fire, and for comparing their performances to those in shielded fire scenarios.

The fire was allowed to burn freely for approximately 12 minutes during test until the gasoline in the pan was burnt out. The fire developed very quickly to reach its maximum heat release rate (100~125 kW) (Figure 6.1). The rise rate of the ceiling temperature above the fire source was approximately 15°C/min. The maximum ceiling temperature above the fire source was approximately 22°C. The small amount of dark smokes was generated and accumulated below the ceiling. They didn't obstruct the visual view of CCTV detectors to monitor the fire conditions during test.



Figure 6.1. An open space gasoline pool fire in the test tunnel

As shown in Table 6.1, all the optical flame and CCTV detectors responded quickly to this small and open gasoline pool fire. Their detecting times were less than 15 s. The linear fiber optic heat detection system D-1L1 also detected the fire at 22 s as the ceiling temperature quickly raised. The smoke detection system detected the fire at approximately 103 s. There was no response from the linear heat detection system D-2L2 and two spot heat detectors as the ceiling temperature during test was below to their presetting alarm thresholds.

6.1.2 Pool Fires underneath the Vehicle

The fire scenarios were designed for simulating tunnel fire incidents in which two vehicles crashed together, and the fuel leaked from the backward vehicle and generated a gasoline pool fire underneath the vehicle. As shown in Figure 6.2, a pool pan was placed underneath a simulated vehicle. It had a similar bottom area (1.5 m (5 ft) wide by 2.4m (8 ft) long) as a standard passenger vehicle. The gap between the bottom of the simulated vehicle and the ground was 0.3 m. A plate with a size of 1.5 m (5 ft) wide by 1.2 m (4 ft) high, simulating a crashed car located between the fire source and the wall-mounted detectors, was placed 1.5 m in front of the fire source and 0.3 m (1 ft) above the ground.

During tests, the fire source was located at the same place as in the test involving an open space fire in test T-1. Six fire tests with various fire sizes and two fuel types were conducted to evaluate performances of detectors/detection systems in response to various sizes of fires underneath the vehicle. The test conditions and results were listed in Table 6.1.



Figure 6.2. Schematic of the setup for a fire underneath a vehicle

Table 6.1. Test Conditions and Results in Pool Fire Scenarios

FIRE SCENARIO	TEST NO	FIRE SOURCE	FUEL TYPE	HEAT RELEASE RATE (KW)	T_{ROOM} (°C)	D-1L1 (S)	D-2L2 (S)	D-3F1 (S)	D-4C1 (S)	D-5C2* (S)	D-6C3 (S)	D-7H1 (S)	D-8H2 (S)	D-9S1 (S)
Open fire	T-1	0.3 x 0.3	Gasoline	100 ~ 125	6	24	N/A	4	14	10	9	N/A	N/A	103
Fire under the vehicle	T-2	0.3 x 0.3	Gasoline	100 ~ 125	6	N/A	N/A	N/A	125	N/A	N/A	N/A	N/A	133
	T-3	0.6 x 0.6	Gasoline	550 ~ 650	6	37	75	26	29	44	N/A	N/A	N/A	50
	T-7	1.0 x 1.0	Gasoline	1500 ~ 1700	1	26	51	6	10	17	28	231	125	47
	T-15	1.0 x 2.0	Gasoline	3000 ~ 3400	13	17	26	4	156	13	38	183	101	86
	T-16	Burner	Propane	1500 ~ 1700	13	22	35	12	15	N/A	195	152	72	N/A
	T-18	Burner	Propane	3000 ~ 3400	9	25	27	3	8	14	N/A	31	36	N/A
Fire behind the vehicle	T-8	0.3 x 0.3	Gasoline	100 ~ 125	5	43	N/A	22	19	24	N/A	N/A	N/A	125
	T-9	0.6 x 0.6	Gasoline	550 ~ 650	5	30	58	12	127	16	N/A	N/A	N/A	52
	T-10	1.0 x 1.0	Gasoline	1500 ~ 1700	10	10	21	8	32	N/A	N/A	62	37	38
	T-11	1.0 x 2.0	Gasoline	3300 ~ 3400	12	20	14	8	26	16	N/A	20	19	33

Note:

- No testing data from Detecting System D-5C2 were collected by the project data acquisition system, because of technical malfunction of System D-5C2. The test data of System D-5C2 that are listed in Table 7.1 were provided by the system supplier after the tests, which are not verified by the project.
- The systems listed in the table are:
 - 1) D-1L1: Linear fiber optic heat detection system
 - 2) D-2L2: Linear analogue heat detection system
 - 3) D-3F1: Optical flame detector
 - 4) D-4C1: CCTV flame/smoke detector
 - 5) D-5C2: CCTV flame detector
 - 6) D-6C3: CCTV flame detector
 - 7) D-7H1: Spot heat detector
 - 8) D-8H2: Spot heat detector
 - 9) D-9S1: Smoke detection system

For the tests involving gasoline fuel, four pans with sizes of 0.09 m², 0.36 m², 1.0 m² and 2.0 m² were placed underneath the vehicle, respectively. The fire in test T-2 involving 0.09 m² gasoline pan was allowed to burn freely for approximately 8 minutes. The fire size was small, and the flame was confined underneath the vehicle but the smoke escaped from the vehicle, as shown in Figure 6.3. The maximum ceiling temperature above the fire source was approximately 13°C. The rise rate of the ceiling temperature above the fire source was approximately 5°C/min. Both maximum ceiling temperature and its rise rate were lower than those generated from an open gasoline pool fire in test T-1 with the same size of the pan.



Figure 6.3. A 0.3 m x 0.3 m gasoline pool fire underneath the vehicle in test T-2

Only visual flame and smoke CCTV detector D-4C1 and smoke detection system D-9S1 detected the fire at 125 s and 133 s, respectively, as they responded to the smoke released from the fire. Their detecting times were longer than those in the open space fire. All other fire detectors/detection systems had no response to the fire in test T-2.

With an increase in the pool size, the fire size increased and more flames and smokes were generated and stretched outside the vehicle, as shown in Figure 6.4 with a large gasoline pool fire (1.0 m²) in test T-7. The heat flux measured at different locations of the tunnel in test T-7 are shown in Figure 6.5. It indicates that once ignited, the gasoline pool fire developed very quickly. The heat flux continuously increased with time until the fire was extinguished at 5:50 minutes after ignition. The maximum heat flux measured at 1 m from the fire source was approximately 19 kw/m² and it decreased with an increase in distance from the fire.



Figure 6.4. Tunnel conditions with a gasoline pool fire (1.0 m x 1.0 m) underneath the vehicle in test T-7

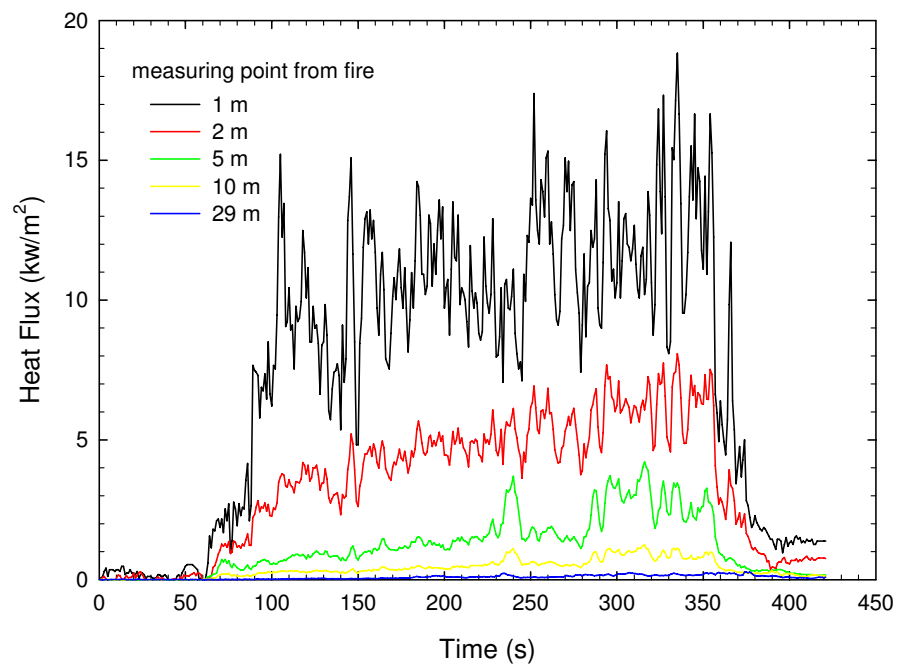


Figure 6.5. Variations of heat flux with distance from the fire source in Test T-7 with a 1.0 m by 1.0 m gasoline pool fire underneath the vehicle

Figure 6.6 shows variation of temperatures measured above the fire source with time in test T-7. The maximum temperature measured at 0.6 m above the ground was approximately 900°C and it declined with an increase in distance from the fire source. The temperatures measured above 2.8 m from the ground did not show substantial decrease with an increase in distance from the fire source. The temperature measured at the middle point of the tunnel showed different trend from those measured above the fire source (Figure 6.7). Its temperatures increased with time and with an increase in the elevation from the ground. The maximum temperature measured at 5 m from the ground was nearly 95°C.

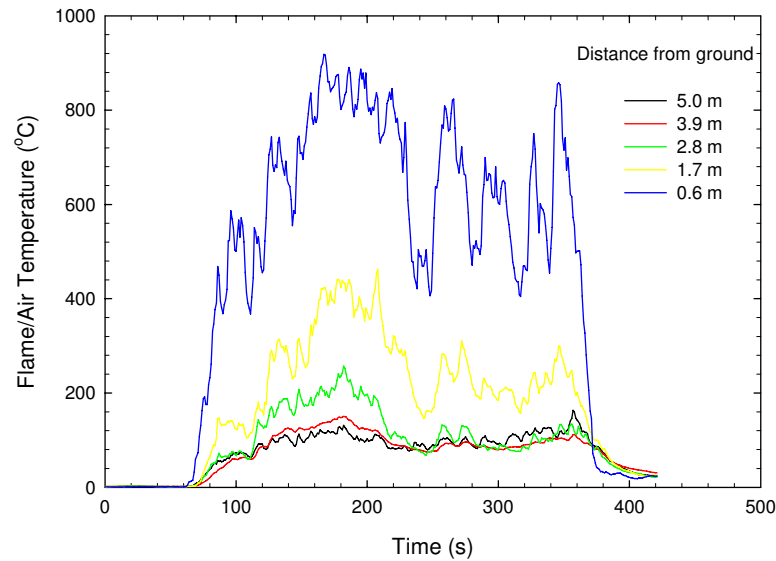


Figure 6.6. Flame and air temperatures above the fire source in Test T-7 with a 1.0 m by 1.0 m gasoline pool fire underneath the vehicle

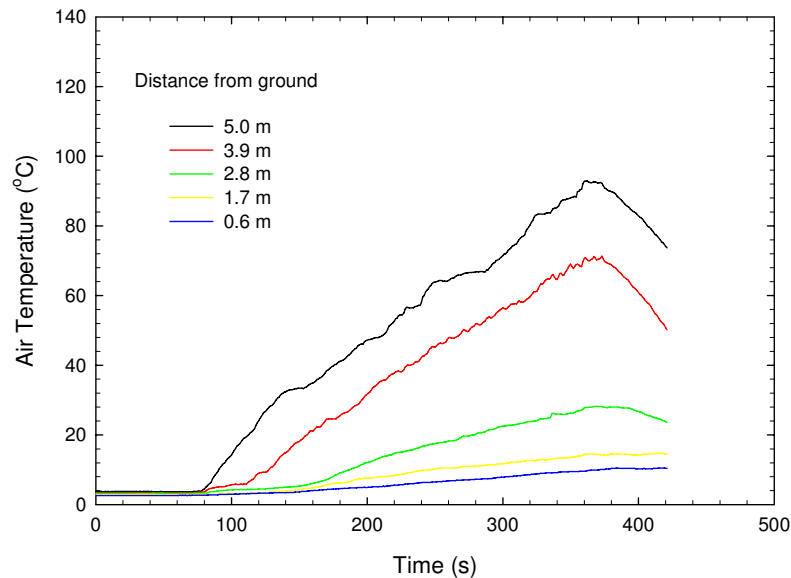


Figure 6.7. Variation of air temperatures along elevation at the middle of the tunnel in Test T-7 with a 1.0 m by 1.0 m gasoline pool fire underneath the vehicle

Figure 6.8 shows the variation of ceiling temperatures along the center of the tunnel in test T-7. They increased quickly with time and decreased with an increase in distance from the fire source. The maximum temperatures measured at center of the tunnel were approximately 125°C near the fire source. Figure 6.9 shows changes in the ceiling temperatures across the tunnel measured near the fire source (6.2 m from east end of the tunnel). They also have substantial decrease with an increase in distance from the fire source. The maximum ceiling temperature near the fire source was approximately 170°C.

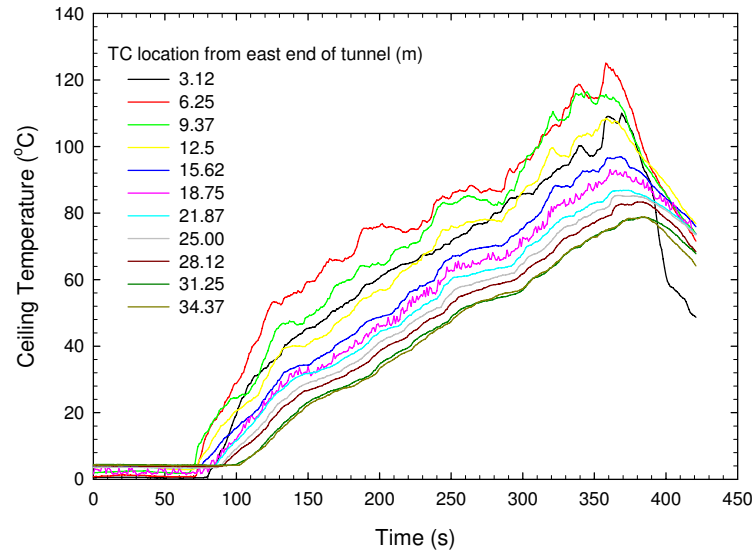


Figure 6.8. Ceiling temperatures along center of the tunnel in Test T-7 with a 1.0 m by 1.0 m gasoline pool fire underneath the vehicle

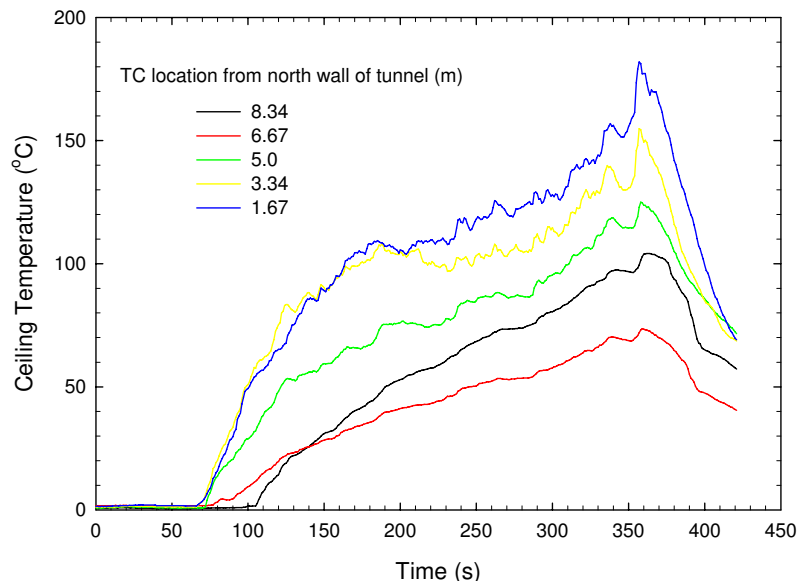


Figure 6.9. Ceiling temperatures across the tunnel near the fire source in Test T-7 with a 1.0 m by 1.0 m gasoline pool fire underneath the vehicle

Temperature distributions in the tunnel at 2 minutes after ignition are shown in Figure 6.10. It suggests that the fire had substantial impact on the ceiling temperature in the area with radius of 5 m from the fire source. The changes in ceiling temperatures across the tunnel tended to become small as the distance to the fire source increased. Figure 6.10 also showed that the ceiling temperatures near to partially opening side louver at the east end of the tunnel and near to partially opening side door at the west end of the tunnel substantially dropped, in comparison to temperatures located at other areas, indicating air exchange between inside and outside of the tunnel.

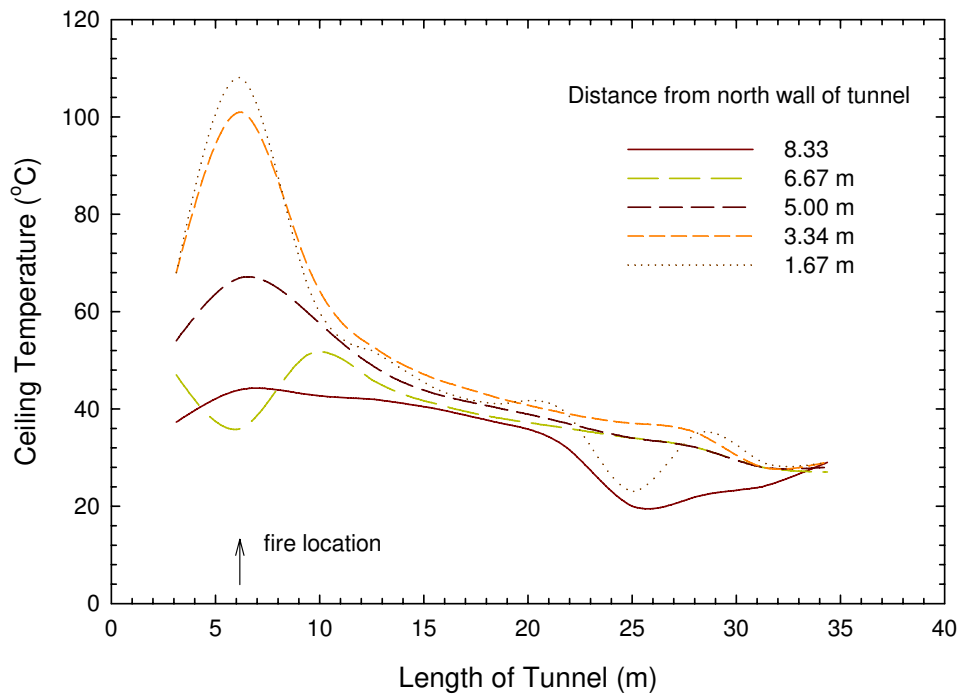


Figure 6.10. Ceiling temperature distribution in the tunnel at 2 minutes after ignition in Test T-7 with a 1.0 m by 1.0 m gasoline pool fire underneath the vehicle

Figure 6.11 further shows that variation of smoke density measured at the middle of the tunnel with time in test T-7. The smoke density at 15 cm below the ceiling increased slowly at initial stage of the fire, and then quickly increased from 170 s after ignition. The smoke densities measured at 2.5 m and 3.97 m below the ceiling were not very high, and increased slowly with time. There was no air velocity in the tunnel.

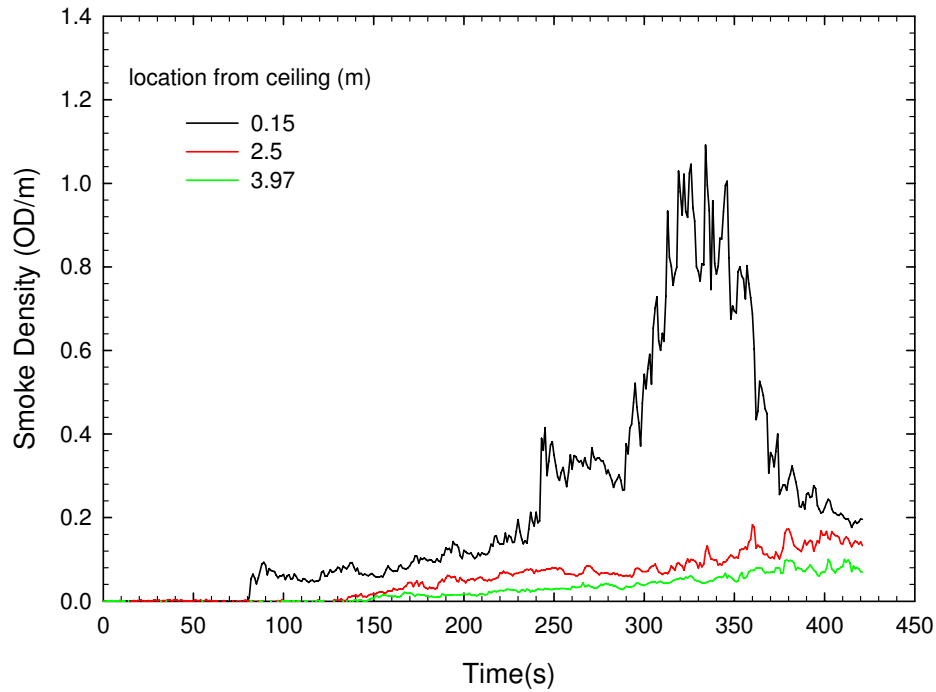


Figure 6.11. Variations of smoke density below the ceiling at center of the tunnel in Test T-7 with a 1.0 m by 1.0 m gasoline pool fire underneath the vehicle

Figures 6.12 to 6.15 compare the changes in the heat flux measured at 1 m from the fire source, and smoke density measured at 15 cm below the ceiling, and the maximum ceiling temperatures along the center of the tunnel and across the tunnel near the fire source, when four gasoline pool pan sizes were used in the test series. The heat flux, smoke density and ceiling temperatures increased with an increase in pan size from 0.09 m² to 1.0 m². However, when further increase in pan size from 1.0 m² to 2.0 m², its both heat flux and smoke density were lower than those with gasoline pan size of 1.0 m², and its maximum ceiling temperatures were also lower than those with the gasoline pan size of 1.0 m², indicating that the combustion of 2.0 m² gasoline pool fire underneath the vehicle was not fully developed, as available oxygen for the combustion of the fire was limited by the existence of the vehicle body above the pool pan.

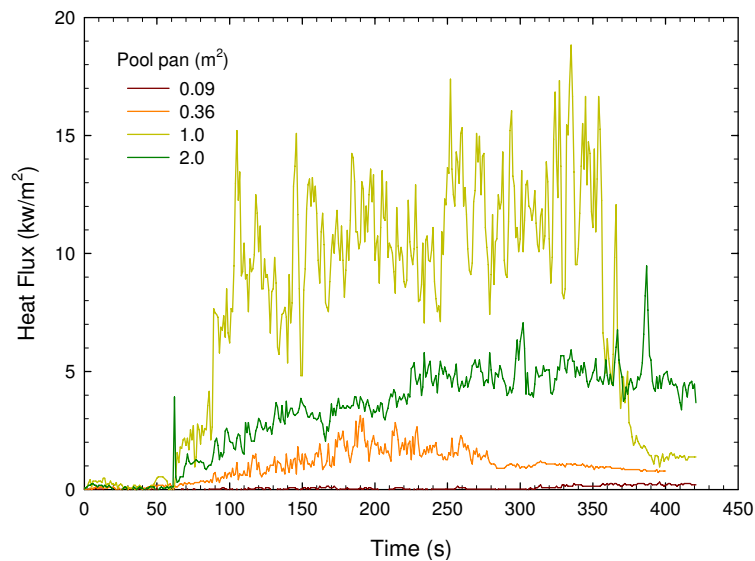


Figure 6.12. Heat flux measured with four gasoline pool pans underneath the vehicle

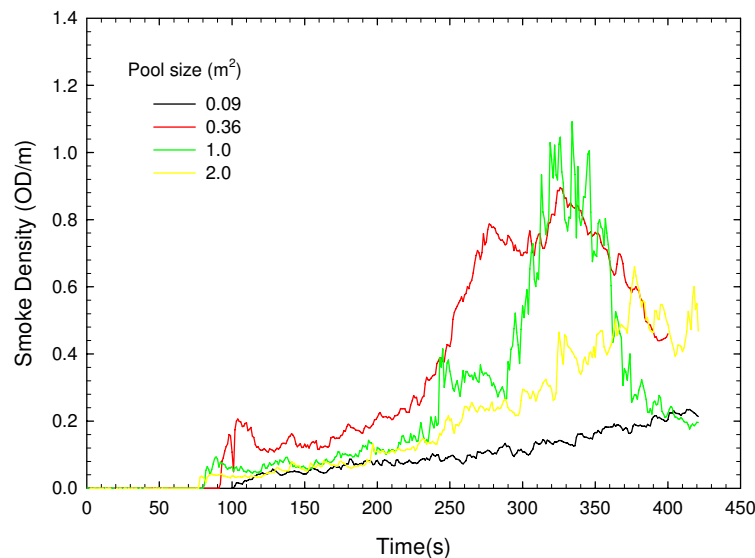


Figure 6.13. Smoke densities measured with four gasoline pool pans underneath the vehicle

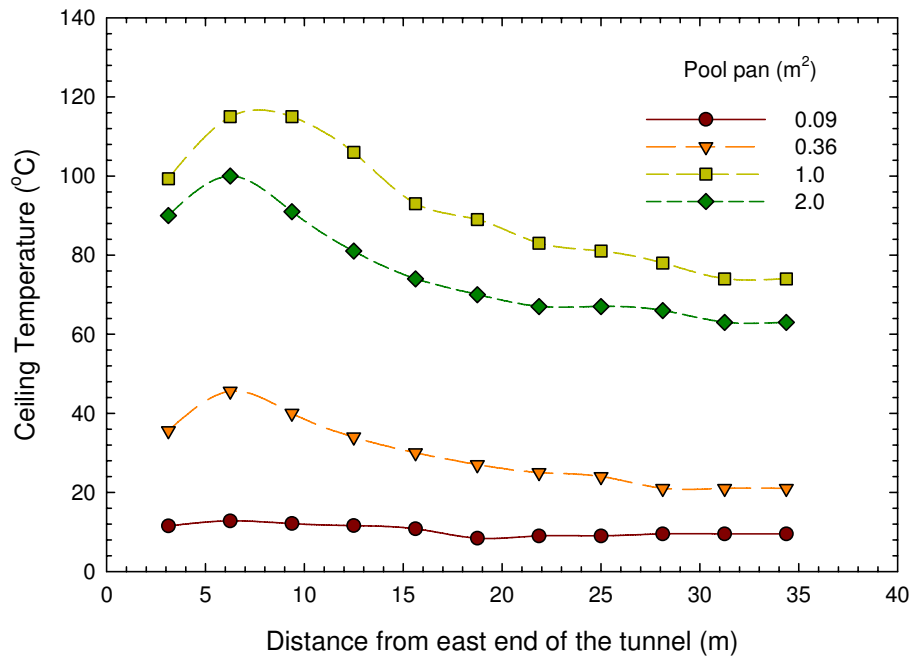


Figure 6.14. Maximum ceiling temperatures along center of the tunnel with four gasoline pool pans underneath the vehicle

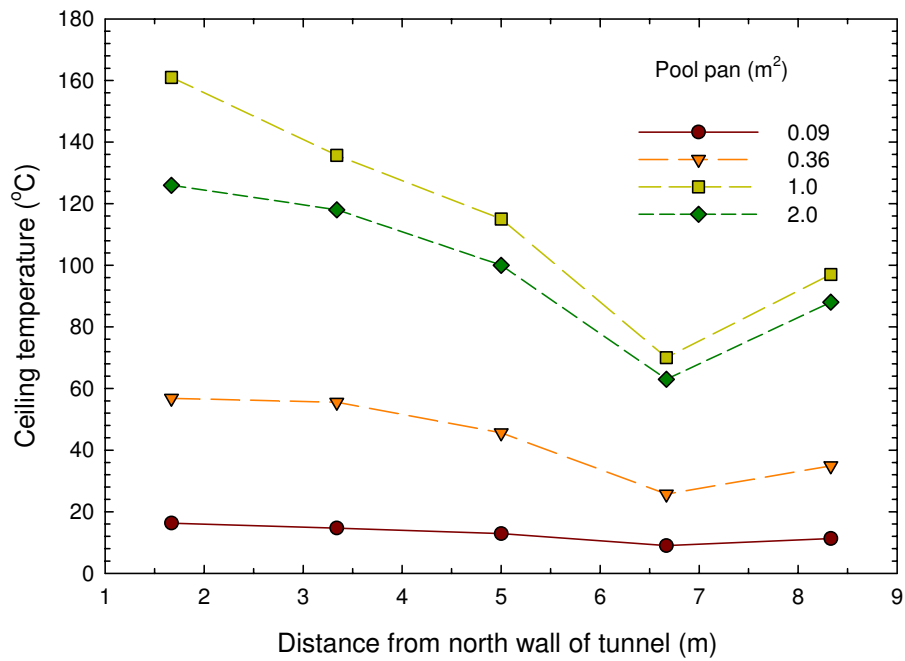


Figure 6.15. Maximum ceiling temperatures across the tunnel near fire with four gasoline pool pans underneath the vehicle

During tests, the linear heat detection system D-1L1 could not detect the fire underneath the vehicle with a 0.09 m² gasoline pool fire, but it detected all other three large gasoline fires in less than 40 s, as shown in Table 6.1. Its detecting time decreased with an increase in fire size. The detecting time was 35 s for the 0.36 m² gasoline pool fire, and then decreased to 17 s for the 2.0 m² gasoline pool fire. System D-1L1 was also able to provide information on the variation of temperatures along its optical linear cable with time, as shown in Figure 6.16 with 0.36 m² gasoline pool fire in test T-3. The system quick responded to the change in temperature, and the position in which the temperature has a sharp increase is the location close to the fire source.

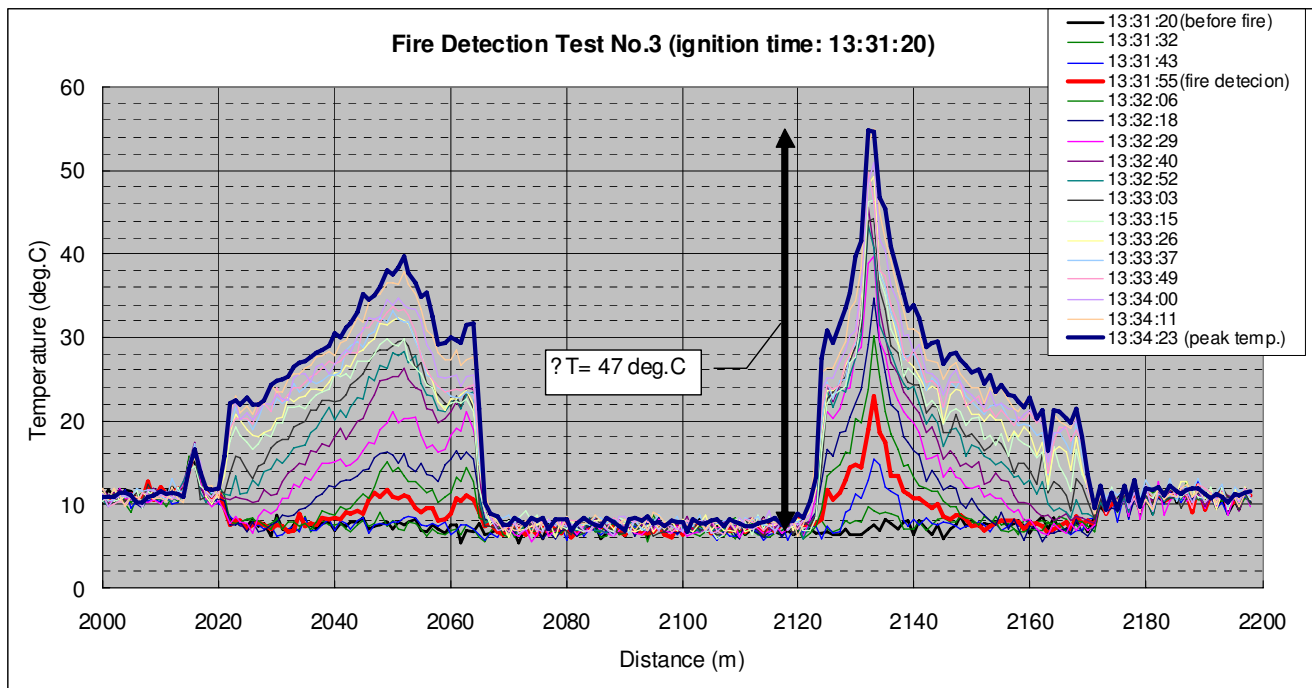


Figure 6.16. Variations of temperatures along the cable with time in test T-3 with a 0.36 m² gasoline pool pan underneath the vehicle

The linear heat detection system D-2L2 also did not detect a 0.09 m² gasoline pool fire. It detected all other three large gasoline fires ranging from 75 s to 26 s. Its detecting time decreased with an increase in fire size.

The optical flame detector D-3F1 did not detect a 0.09 m² gasoline pool fire, but it detected other three large gasoline fires very quickly, ranging from 26 s to 4 s. Its detecting time also decreased with an increase in fire size.

The visual CCTV flame and smoke detector D-4C1 detected all the four gasoline pool fires underneath the vehicle ranging from 156 s to 10 s, based on characteristics of smoke and flame generated from fires. Its detecting time generally decreased with an increase in fire size, but its detecting time for the 2.0 m² gasoline pool fire was even longer than that with 0.09 m² gasoline pool fire. One explanation for this phenomenon was that the flame burst from the 2.0 m² gasoline pool fire after ignition was much larger than presetting alarming thresholds of the system, and it took a long time for the system to reset its response.

The visual camera was able to provide video images on fire conditions in the tunnel during entire test with 0.09 m² gasoline pool fire. Visual view of the camera to the tunnel, however, could be completely shut during tests with an increase in fire size, as the smoke density in the hot layer increased. The time for completely shutting visual view of the camera due to smoke was approximately 3:30 minutes for 0.36 m² gasoline pool fire, 3:45 minutes for 1.0 m² gasoline pool fire, and 4:40 minutes for 2.0 m² gasoline pool fire. This was consistent with smoke density measured in tests. As shown in Figure 6.13, smoke density generated in the fire with 0.36 m² gasoline pool is higher than those in two fires with large gasoline pools at initial 5 minutes of fire development.

The visual CCTV flame detector D-6C3 could not detect two small underneath fires, but responded to two large fires in less than 40 s.

Both spot heat detectors D-7H1 and D-8H2 only responded to two large underneath fires. Their detecting times declined with an increase in pool pan size. For a 2.0 m² gasoline pool fire underneath the vehicle, the detecting times of two detectors were 183 s and 101 s.

The smoke detection system D-9S1 detected all the four underneath gasoline fires ranging from 133 s to 47 s, based on characteristics of smoke generated from the fires. Its detecting time decreased with an increase in the fire size, but its detecting time for the fire with 2.0 m² pan was extended and longer than that in the fire with 0.36 m² pan. This was consistent with smoke density measured in tests. As shown in Figure 6.13, the smoke density measured in the fire with 2.0 m² pan was lower than that measured in the fire with 0.36 m² pan due to its incomplete combustion.

During tests, the propane burner was used to simulate large pool fires underneath the vehicle. The setup of the fire scenarios was the same as those with gasoline pool fires. Two tests with different propane fire sizes (tests T-16 and T-18) were conducted. As shown in Figure 6.17 with a propane fire in test T-16, the fire generated from the propane burner is similar to the fire generated from a underneath gasoline pool, when it is viewed from the front of the simulated vehicle. However, no smoke was generated from propane fires.

The heat release rate generated from the propane burner in two tests was controlled manually to simulate those generated from underneath gasoline pool fires, based on previous calibration tests [2]. Figure 6.18 shows variation of ceiling temperatures with time in tests T-7 and T-16 with gasoline and propane fires. The temperatures were measured at thermocouple #28 located at the center of the tunnel ceiling in two tests. For the similar heat release rate, the temperature generated in two tests had a similar developing trend and their maximum temperatures were also close.

During two tests involving propane fires, the smoke detecting system D-9S1 had no response to the propane fires due to no smoke in the tunnel. The visual CCTV flame detector D-6C3 had difficulty to detect the propane fires. It detected the fire with 1,500 kW at 195 s in test T-16 and could not detect the large fire with 3,000 kW in test T-18. All other detectors/detection systems were able to detect the propane fires. Their detecting time decreased with an increase in propane fire size. Compared to the same setup with a 1.0 m² gasoline pool fire in Test T-7, the detecting time for the 1,500 kW propane fire in Test T-16 was reduced for linear heat detection systems D-1L1 and D-2L2, and for two spot heat detectors (D-7H1 and D-8H2), but slightly increased for the optical flame detector D-3F1 and the visual CCTV flame and smoke detector D-4C1. The sensing cable of the linear heat detection system D-2L2 was damaged in Test T-18, after the maximum ceiling temperature was higher than 240°C.



a). Side view of a underneath propane fire



b). Front view of a underneath propane fire

Figure 6.17. A propane fire (1,500 kW) in test T-16

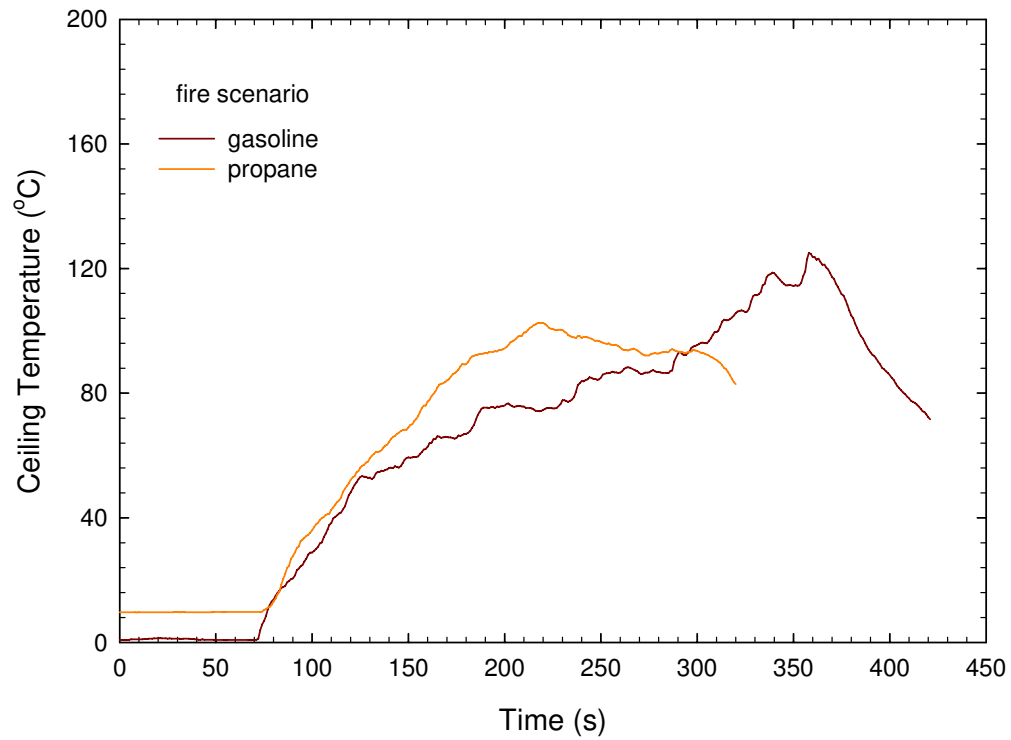


Figure 6.18. Ceiling temperatures measured at Thermocouple #28 at center of the tunnel ceiling in test T-7 with gasoline fuel and in test T-16 with propane fuel

6.1.3. Open Pool Fires behind a Large Vehicle

The fire scenarios were designed for simulating tunnel fire incidents in which an open gasoline pool fire was formed behind a large vehicle due to the crash or mechanical failure of the vehicle. The fire scenario was constructed by placing an open pan fire behind a large plate. The plate had a size of 2.5 m (8.3 ft) wide by 3.5 m (11.7 ft) high, being representative of the size of a large truck. It was placed 0.3 m (1 ft) above the ground, and 6 m (20 ft) in front of the pool fire, simulating the front portion of a crashed truck located between the pool fire and the detectors. The distance between the edge of the plate and the wall of the tunnel was 1.2 m (4 ft). The schematic of an open pool fire located behind a large vehicle and overview of its setup are shown in Figures 6.19 and 6.20.

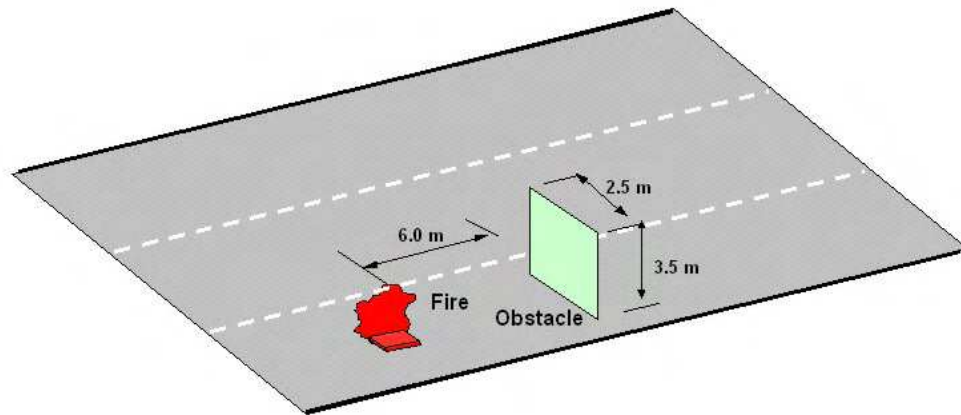


Figure 6.19. Schematic of the setup for a pool fire behind a vehicle



Figure 6.20. Overview of the setup for a pool fire behind a vehicle

Four tests with gasoline pool fires ranging from 125 kW to 3,400 kW were conducted. Four pans with sizes of 0.09 m², 0.36 m², 1.0 m² and 2.0 m² were placed behind the large plate, respectively. The gasoline pool fire behind the vehicle was a freely burning fire with sufficient air supply. It developed very quickly and generated a hot smoke layer below the ceiling, as shown in Figure 6.21 with a 1.0 m² gasoline pool fire in test T-10.



Figure 6.21. A 1.0 m² gasoline pool fire behind a large vehicle



Figure 6.22. Front view of a 0.09 m² gasoline pool fire behind a large vehicle (T-8)

However, it was difficult to view the flames from front of the large vehicle. When the fire was small, the flame was not big enough to stretch out from behind of the vehicle, and the flame could only be observed from the gap between the bottom of the vehicle and the ground (Figure 6.22). With an increase in fire size, the flame became big and high, and it flickered out from behind of the large vehicle, as shown in Figure 6.23a with a 2.0 m² gasoline pool fire in test T-11. However, as shown in Figure 6.23b, the smoke layer quickly formed and descended from the ceiling within a short period of time, which blocked the view to the flames from front of the large vehicle.



a). A 2.0 m² gasoline pool fire behind a large vehicle at 10 s after ignition



b). A 2.0 m² gasoline pool fire behind a large vehicle at 25 s after ignition

6.23. Front view of a 2.0 m² gasoline pool fire behind a large vehicle in test T-11

Figures 6.24 to 6.26 compare the heat flux measured at 1 m from the fire source, the ceiling temperatures measured at 3 m from the fire source, and smoke density measured at 15 cm below the ceiling with the same gasoline pool pan (1.0 m^2) for fires located underneath and behind the vehicle in tests T-7 and T-10. They indicate that fires behind the vehicle develop much faster than fires underneath the vehicle, and generate hotter ceiling temperatures. Also, the hot smoke layer is more quickly built below the ceiling. The tests for fires behind the vehicle were terminated by using a compressed air foam (CAF) system. A substantial increase in fire size and heat release rate was generated as the discharge of foam agitated the combustion of gasoline fire.

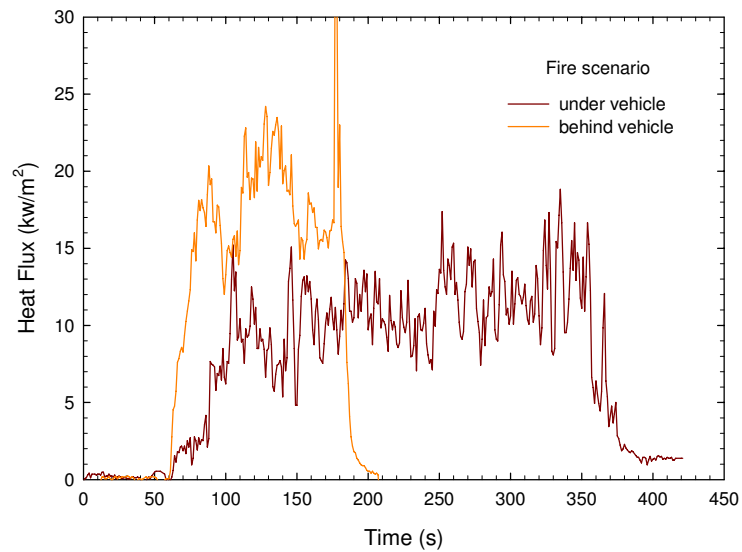


Figure 6.24. Heat flux measured at 1 m from the fire source with a 1.0 m^2 gasoline pool pan at two fire scenarios (tests T-7 and T-10)

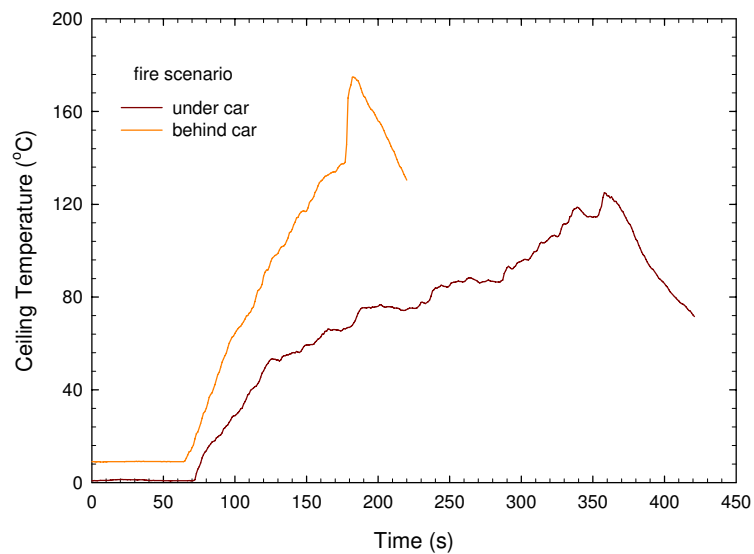


Figure 6.25. Ceiling temperatures measured at 3 m from the fire source with a 1.0 m^2 gasoline pool pan at two fire scenarios (tests T-7 and T-10)

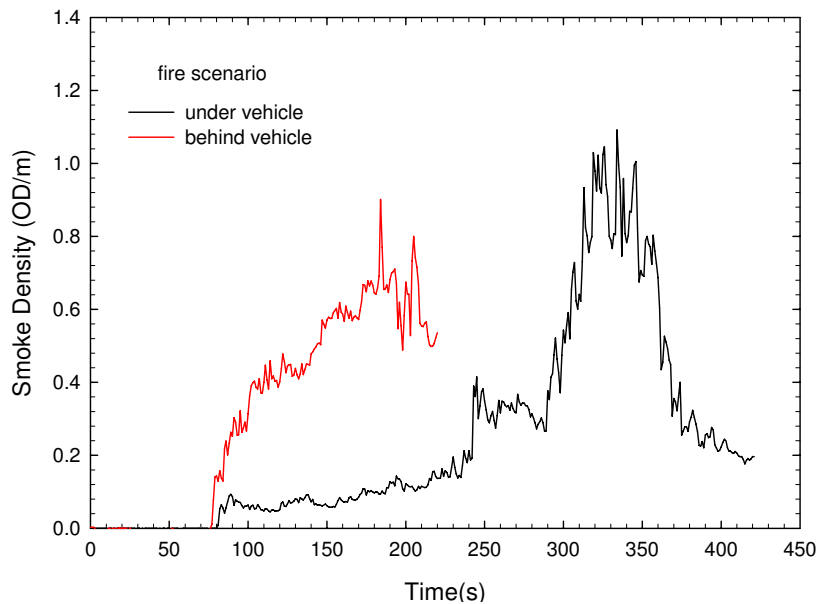


Figure 6.26. Smoke Density measured at 0.15 m below the ceiling at the center of the tunnel with a 1.0 m² gasoline pool pan at two fire scenarios (tests T-7 and T-10)

Figure 6.27 compares the changes in heat flux generated from four fire sizes behind the vehicle in the tests. The large fires not only generated high heat flux and their developing rate also tends to be faster than small fires. It took less than 30 s for the fire with a size of 3,400 kW to reach its maximum heat release rate. In addition, their developing trends were different from those observed in pool fires underneath the vehicle, as shown in Figure 6.12.

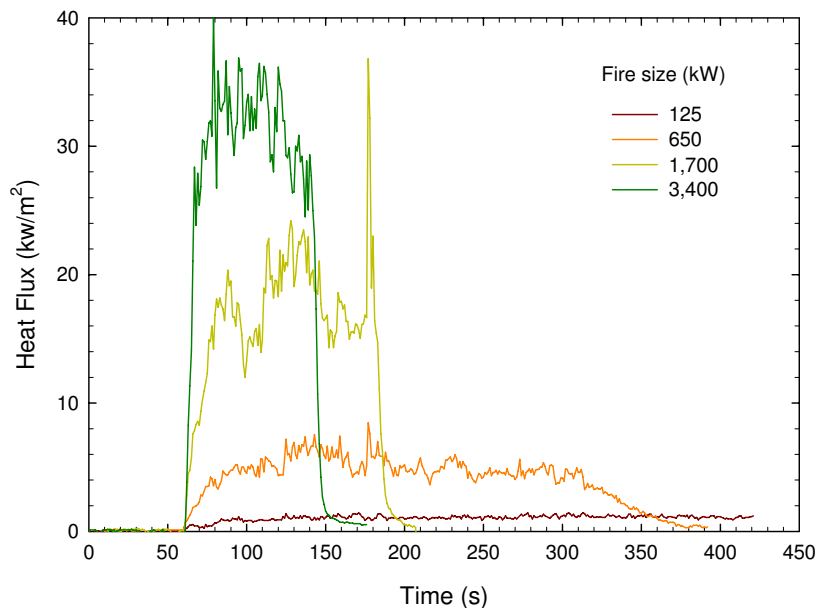


Figure 6.27. Heat flux measured from four pool fires behind the vehicle

Figures 6.28 and 6.29 are maximum ceiling temperatures across the tunnel near the fire source and along the center of the tunnel that were measured from four pool fires behind the vehicle. The ceiling temperatures substantially increased with fire size and the maximum ceiling temperature near the fire source was higher than 400°C for a pool fire of approximately 3,400 kW. The ceiling temperatures across the tunnel and along the center of the tunnel quickly dropped with an increase in distance from the fire source. Their drops in temperature tended to increase with an increase in fire size. For example, the drop in the maximum ceiling temperature between two locations (1.6 m and 5.0 m to north wall of the tunnel) across the tunnel was from 419°C to 257°C for the fire of 3,400 kW and from 209°C to 138°C for the fire of 1,700 kW.

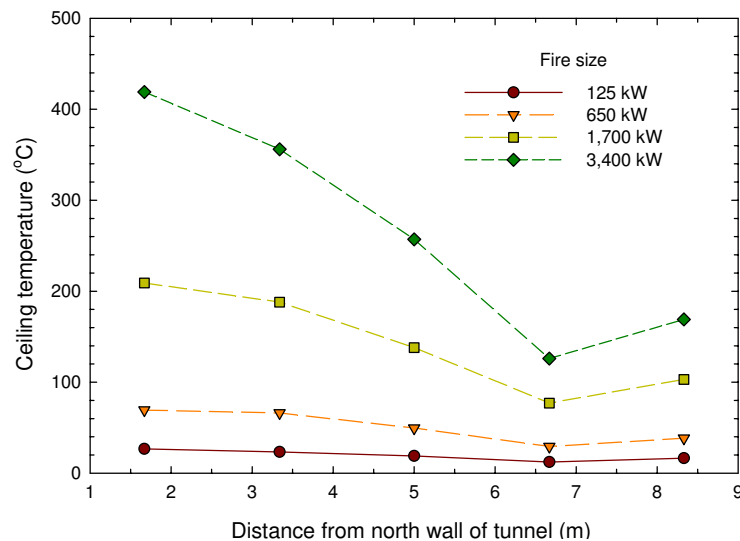


Figure 6.28. Maximum ceiling temperatures across the tunnel measured near the fire source in four pool fires behind the vehicle

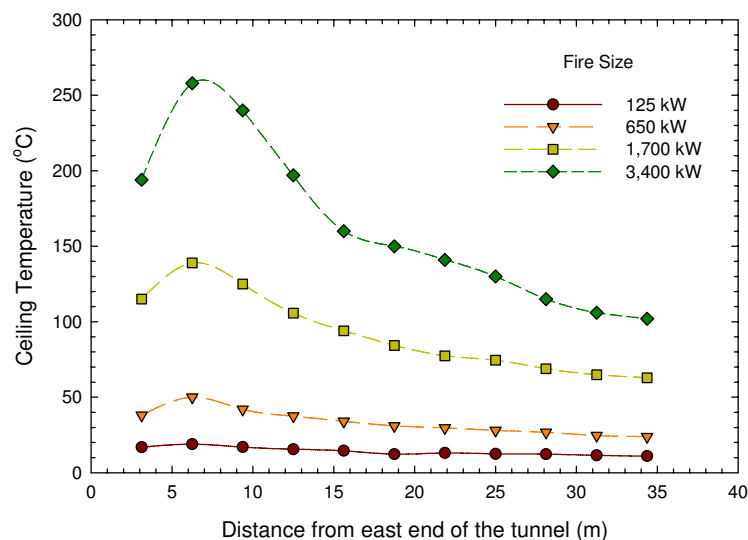


Figure 6.29. Maximum ceiling temperatures along center of the tunnel measured in four pool fires behind the vehicle

Figure 6.30 further shows changes in smoke density measured at 15 cm below the ceiling in four pool fires behind the vehicle. With an increase in fire size, not only the smoke density generated substantially increased, but also the smoke spread in the tunnel speeded up. As indicated in Figure 6.30, it took approximately 40 s after ignition for the smoke generated from the fire of 125 kW to reach the center point of the tunnel, but only approximately 15 s for the smoke generated from the fire of 3,400 kW to reach the same location.

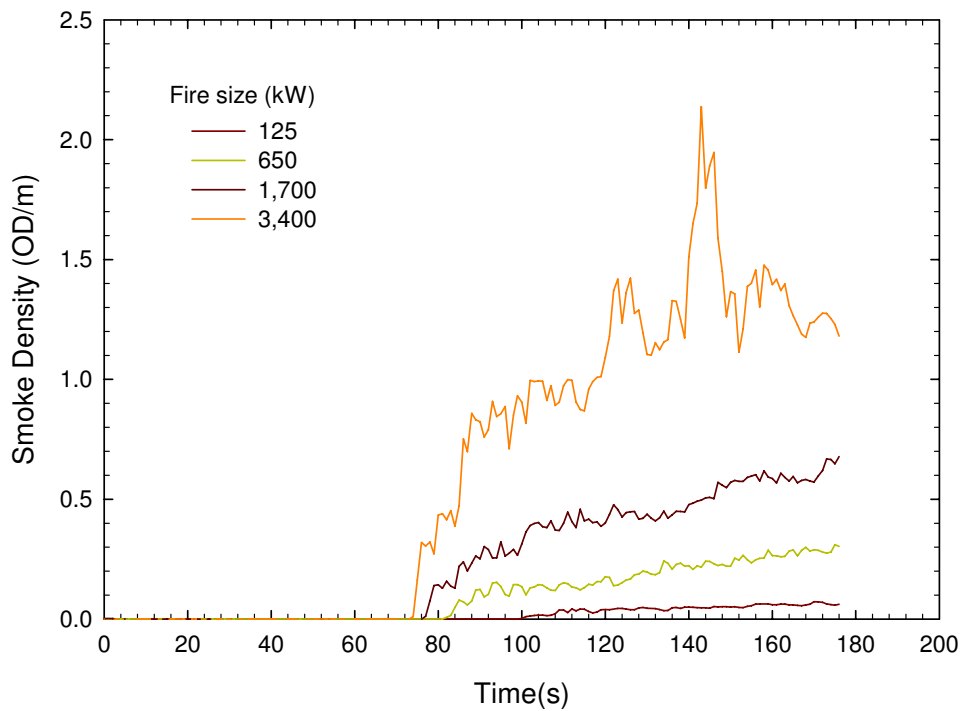


Figure 6.30. Smoke density generated in four pool fires behind the vehicle

During tests, linear heat detection system D-1L1 detected all the four fires behind the vehicle ranging from 43 s to 10 s. Its detecting time decreased with an increase in fire size. Linear heat detection system D-2L2 could not detect a small fire with a 0.09 m² gasoline pool, but it detected all other three fires ranging from 58 s to 14 s. Its detecting time also decreased with an increase in fire size. As shown in Table 6.1, the detecting times of both linear heat systems for fires behind the vehicle were shorter than their detecting times for fires underneath the vehicle. The sensing cable of the linear heat detection system D-2L2 was damaged in test T-11 with 2.0 m² gasoline pool fire, after the maximum ceiling temperature reached beyond 400°C.

Optical flame detector D-3F1 quickly detected all the four fires ranging from 22 s to 8 s. The detecting time decreased with an increase in fire size.

Visual CCTV flame and smoke detector D-4C1 detected all the four fires in tests. Its detecting time was 19 s for the 0.09 m² gasoline pool fire, but increased to 127 s for the 0.36 m² gasoline pool fire, and then reduced to 26 s for the 2.0 m² gasoline pool with an increase in fire size.

The visual camera was able to provide video images on fire conditions in the tunnel during 6 minutes long of the test period with 0.09 m² gasoline pool fire. When the fire size increased, the period of time available for monitoring the tunnel conditions decreased, as the smoke density in the hot layer increased. The time for completely shutting visual view of the camera due to smoke was approximately 3 minutes for 0.36 m² gasoline pool fire, 1:28 minutes for 1.0 m² gasoline pool fire, and 34 seconds for 2.0 m² gasoline pool fire. They were much shorter than those in the fires underneath the vehicle.

Visual CCTV flame detector D-6C3 had no response for four gasoline pool fires behind the vehicle.

Both spot heat detectors D-7H1 and D-8H2 only responded to two large fires with 1.0 m² and 2.0 m² gasoline pans, as they did in fires underneath the vehicle. This was consistent with temperatures measured in the tests. As shown in Figure 6.29, the maximum ceiling temperatures at the center of the tunnel that were generated in fires with 0.09 m² and 0.36 m² gasoline pans were lower than those alarming levels of two spot heat detectors. However, their detecting times were much shorter than those in detecting fires underneath the vehicle. They both detected a 2.0 m² gasoline pool fire around 20 s.

Smoke detection system D-9S1 detected all the four gasoline fires behind the vehicle ranging from 125 s to 33 s. Its detecting time decreased with an increase in the fire size and was slightly shorter than those in tests involving fires underneath the vehicle, particularly for the 2.0 m² gasoline pool fire. The fire behind the vehicle developed quickly, resulting in a short detecting time.

6.2. Stationary Vehicle Fires

Two types of stationary vehicle fire scenarios were used in the test program: an engine compartment fire and a passenger compartment fire. The fire scenarios were designed to simulate fire incidents in which the fire ignited from either engine compartment or passenger compartment of the vehicle due to the crash or mechanical failure of the vehicle. Compared to the pool fires, the fires in the engine and passenger compartments of the vehicle developed much slowly due to their fuel type and location [4, 5].

During tests, no obstacle was located between the fire source and the detectors. Fuel materials in tests included gasoline, propane, plastic foam, and wood crib. The performance of fire detectors/detection systems to slowly growing fires was investigated in tests. Test conditions and results in stationary vehicle fire tests are listed in Table 6.2.

6.2.1. Engine Compartment Fires

A simulated vehicle engine compartment with a dimension of 1.5 m (5 ft) wide x 1.2 m (4 ft) long x 0.67 m (2.2 ft) high was built, as shown in Figure 6.31. Two simulated engine compartment fire tests involving two fuel types (T-5 and T-17) were conducted.

For test T-5, a gasoline fuel pan with a movable lid was placed inside the engine compartment. The dimension of the fuel pan was 1.0 m wide x 2.0 m long x 0.2 m high. During test, the size of the opening of the pan gradually increased to simulate the fire growth rate generated from a real vehicle engine compartment fire [2, 4, 5]. The maximum heat release rate generated in the test was approximately 2,000 kW.

For test T-17, the propane burner that had a controlled heat release rate was also used for simulating a vehicle engine compartment fire. Its growth rate and heat release rate during test were similar to those generated from a real vehicle engine compartment fire [4, 5].



Figure 6.31. Overview of the setup for the engine compartment

Table 6.2. Test Conditions and Results in Stationary Vehicle Fire Scenarios

FIRE SCENARIO	TEST NO	FIRE SOURCE	FUEL TYPE	HEAT RELEASE RATE (KW)	T_{ROOM} (°C)	D-1L1 (S)	D-2L2 (S)	D-3F1 (S)	D-4C1 (S)	D-5C2* (S)	D-6C3 (S)	D-7H1 (S)	D-8H2 (S)	D-9S1 (S)
Stationary vehicle fire	T-5	Engine compartment	Gasoline	~2,000	1	107	175	5	76	96	149	391	295	177
	T-17	Engine compartment	Propane	~2,000	9	33	71	5	7	N/A	N/A	338	252	N/A
	T-14	Passenger compartment	Wood crib	1100~1500	13	171	291	173	188	178	271	N/A	N/A	230
	T-19	Passenger compartment	Foam	100	10	105	N/A	76	12	61	N/A	N/A	N/A	115

Note:

- a) No testing data from Detecting System D-5C2 were collected by the project data acquisition system, because of technical malfunction of System D-5C2. The test data of System D-5C2 that are listed in Table 7.1 were provided by the system supplier after the tests, which are not verified by the project.
- b) The systems listed in the table are follows:
 - i. D-1L1: Linear fiber optic heat detection system
 - ii. D-2L2: Linear cable heat detection system
 - iii. D-3F1: Flame detector
 - iv. D-4C1: CCTV flame/smoke detector
 - v. D-5C2: CCTV flame detector
 - vi. D-6C3: CCTV flame detector
 - vii. D-7H1: Spot heat detector
 - viii. D-8H2: Spot heat detector
 - ix. D-9S1: Smoke detection system

During test T-5, the fire gradually grew up and flames stretched outside the engine compartment. It took more than 8 minutes for the fire to become a large one (Figure 6.32). The fire development and smoke spread in the tunnel could be observed clearly, since there was no obstacle around the simulated vehicle.



Figure 6.32. Tunnel conditions during an engine compartment vehicle fire in test T-5

Figure 6.33 shows the heat flux measured at different locations of the tunnel. The fire grew up slowly. It took more than 8 minutes for the fire to reach its maximum heat release rate. The test was terminated by using a compressed air foam (CAF) system. A substantial increase in fire size and heat release rate was generated as the discharge of foam agitated the combustion of gasoline fire.

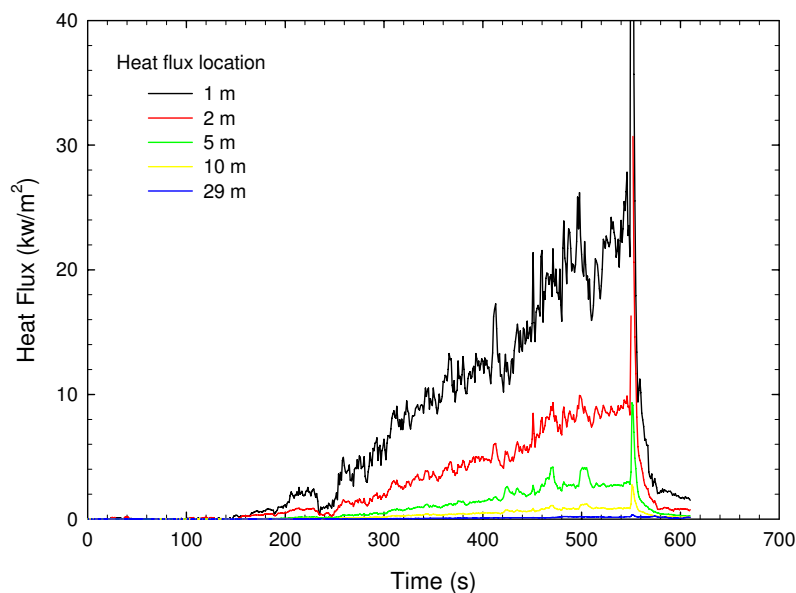


Figure 6.33. Variations of heat flux generated in Test T-5 with an engine compartment fire

The variation of ceiling temperatures along the center of the tunnel and across the tunnel near the fire source in test T-5 is shown in Figures 6.34 and 6.35. The ceiling temperatures increased slowly with time and reached their maximum temperatures of 150°C at the center of the tunnel and 230°C near the fire source after approximately 8 minutes of growing up. The ceiling temperatures further increased as the CAF foam was applied to terminate the test.

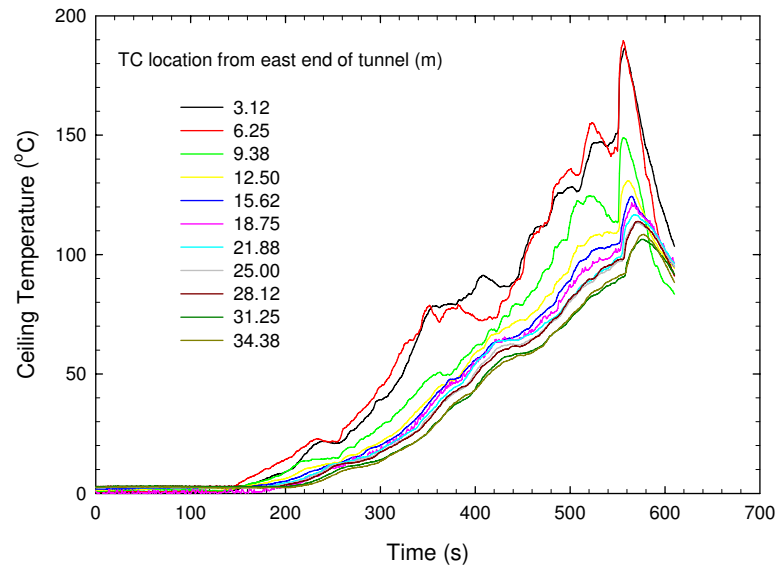


Figure 6.34. Ceiling temperatures along center of the tunnel in Test T-5 with an engine compartment fire

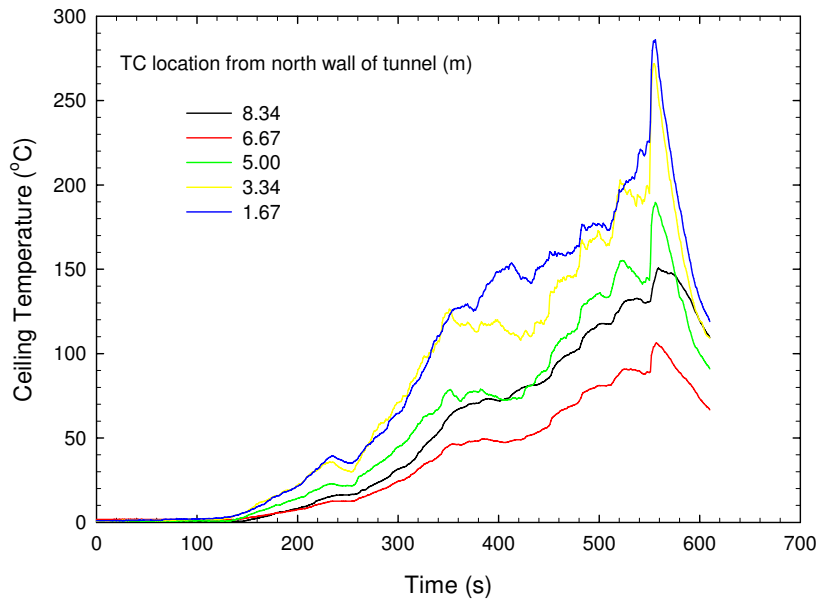


Figure 6.35. Ceiling temperatures across the tunnel near fire source in Test T-5 with an engine compartment fire

Figure 6.36 shows variation of smoke density measured at the middle of the tunnel with time in test T-5. Smoke density in the tunnel also slowly increased. The smoke density at 15 cm below the ceiling was very low at beginning of 2 minutes of the fire growing period, and then gradually increased. The smoke densities measured at 1.53 m and 2.5 m from the ground started to increase approximately 4 minutes after ignition.

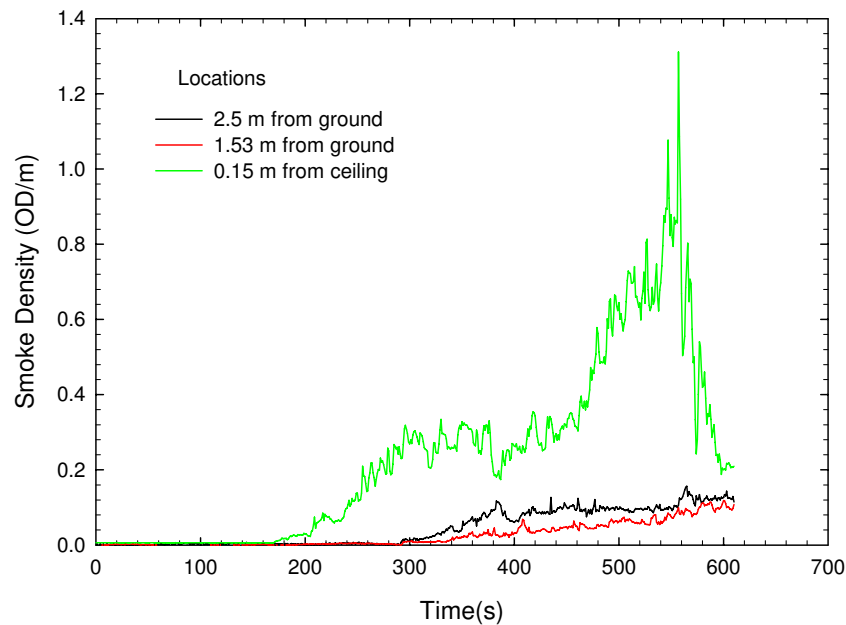


Figure 6.36. Variations of smoke density below the ceiling at center of the tunnel in Test T-5 with an engine compartment fire

The fire detectors/detection systems generally had slow response to the engine compartment fire in test T-5, as the fire grew up slowly. The linear heat detection systems D-1L1 and D-2L2 detected the fire at 107 s and 175 s. Two spot heat detectors D-7H1 and D-8H2 detected the fire at 391 s and 295 s. The smoke detection system D-9S1 also had a slow response to the engine compartment fire at 177 s. Two visual CCTV detectors D-4C1 and D-6C3 detected the fire at 76 s and 149 s. However, the optical flame detector D-3F1 quickly detected flames emitted from the engine compartment at 5 s after ignition.

The fire in test T-17 involving propane fuel also grew up slowly. Flames stretched out from two sides of the engine compartment but no smoke was generated. The response times of linear heat detection systems, spot heat detectors and the visual CCTV detector D-4C1 to the propane fire were shorter than their times to the engine compartment fire with gasoline, as shown in Table 6.2. The response time of the optical flame detector D-3F1 had no changes in two fire tests. However, both visual CCTV detector D-6C3 and the smoke detection system D-9S1 had no response to the fire in the test.

6.2.2. Passenger Compartment Fires

One mock-up simulating the front portion of a vehicle passenger compartment with a dimension of 1.5 m (5 ft) wide x 1.2 m (4 ft) long x 1.2 m (4 ft) high was built. It was assumed that during the fire incident, the door at the driver side of the vehicle was left open, as the driver escaped from the burning vehicle. Two simulated passenger compartment fire tests involving two fuel types (T-14 and T-19) were conducted.

Wood cribs with a dimension of 0.8 m x 0.8 m x 0.7 m and a weight of 62.5 kg were placed inside the compartment in test T-14. Three small pans with 100 ml of methyl hydrate per pan were placed underneath the wood crib in a triangle position. They were used as ignition sources for the wood crib fire. The setup of the passenger compartment fire scenario is shown in Figure 6.37.

The wood crib fire was easily controlled and repeated in the tests. It could generate a fire that had a similar heat release rate and growth rate as those generated in a real vehicle passenger compartment fire [4, 5], when appropriate wood crib size and ignition source were used. The heat release rate of the simulated passenger compartment fire generated by the wood crib fire was measured in Task 1 of the project [2]. Its maximum heat release rate generated in the test was approximately 1,200 kW.

During test T-19, polyurethane foam was used to simulate the smokes and fires generated from the vehicle passenger compartment at its initial fire stage. The dimension of the foam was 0.6 m by 0.6 m by 0.1 m thick and its weight was 1.0 kg, generating a fire with the heat release rate of 100 kW. The combustion characteristics of the polyurethane foam, including its heat release and smoke generation rate, was investigated in a NRC research project [6].



Figure 6.37. Overview of the setup for a passenger compartment vehicle fire

The passenger compartment fire involving wood cribs developed very slowly in test T-14. At its initial fire stage, no visible flame was observed from outside of the compartment and the amount of smoke generated was also limited. After 2 to 3 minutes, the flames started to stretch outside the compartment from its opening door, as shown in Figure 6.38.



Figure 6.38. Passenger compartment fire with wood cribs in test T-14

The development of the passenger compartment fire can be observed from the change in heat flux measured in the test, as shown in Figure 6.39. Approximately 2 minutes after ignition, the heat flux generated by the fire was then large enough to be measured. The fire size started to increase and it took approximately 6 minutes for fire to reach its maximum heat value. The fire size was then remained unchangeable for another 9 minutes period until fuel mass gradually burnt out. The whole test lasted approximately 18 minutes before the fire was extinguished. Compared to the engine compartment fire in test T-5, the passenger compartment fire in test T-14 was smaller and showed a different developing pattern.

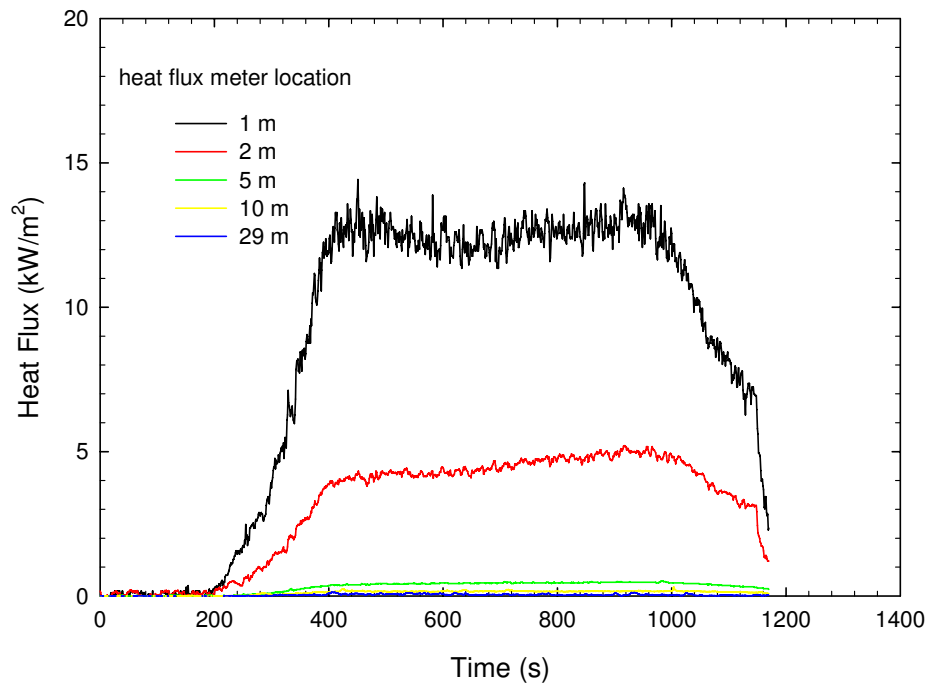


Figure 6.39. Variations of heat flux generated in test T-14 with a passenger compartment fire

Ceiling temperatures in the tunnel had the same developing trend as observed in the heat release rate of the fire. As indicated in Figure 6.40, ceiling temperatures across the tunnel near the fire source started to increase a few minutes late after ignition. The ceiling temperatures did not further increase but remained unchangeable for a long period of time, after reaching its maximum ceiling temperature of approximately 100°C near the fire source. The development of ceiling temperatures along the center of the tunnel had the same trend as those across the tunnel near the fire source, as shown in Figure 6.41. They also remained unchangeable after reaching their maximum temperatures.

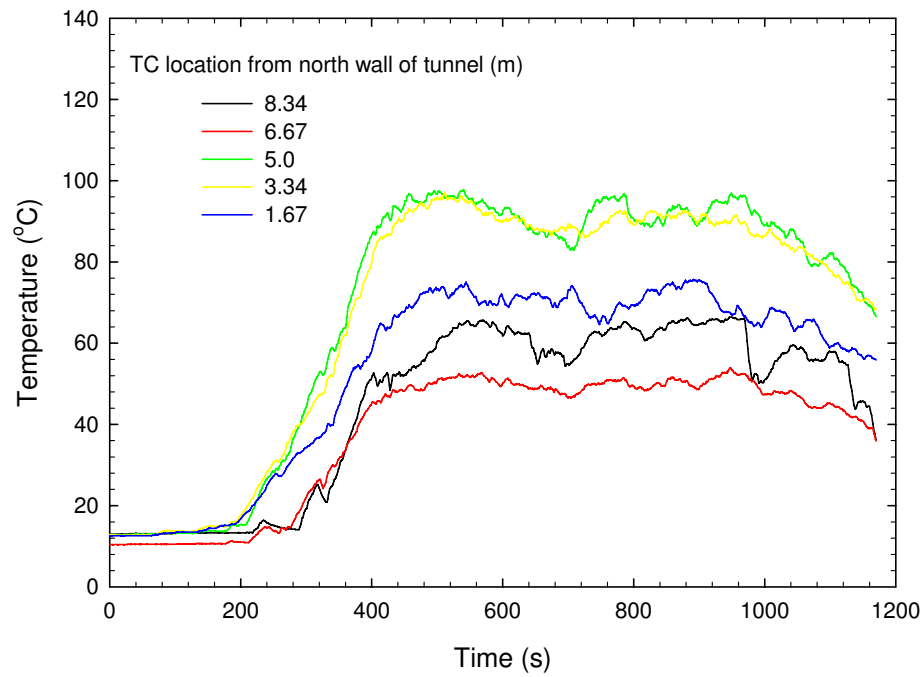


Figure 6.40. Ceiling temperatures across the tunnel near fire source in test T-14

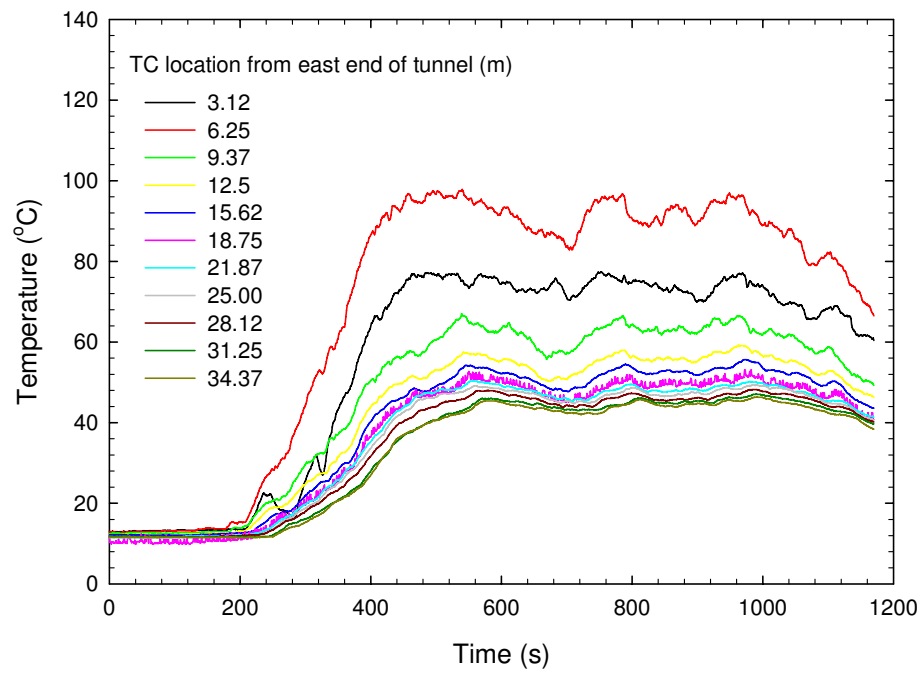


Figure 6.41. Ceiling temperatures along center of the tunnel in test T-14 with a passenger compartment fire

Figure 6.42 shows the variation of smoke density with time measured in test T-14. The smoke density generated in the test was not very high, compared to the engine compartment fire involving gasoline. In addition, difference in smoke density between locations near the ceiling and at low portion of the tunnel was not significant after a certain period of time. This was consistent with the observation in the test in which low dense smoke filled with the entire tunnel and there was not the existence of a distinct hot smoke layer in the tunnel, as observed in other fire scenarios.

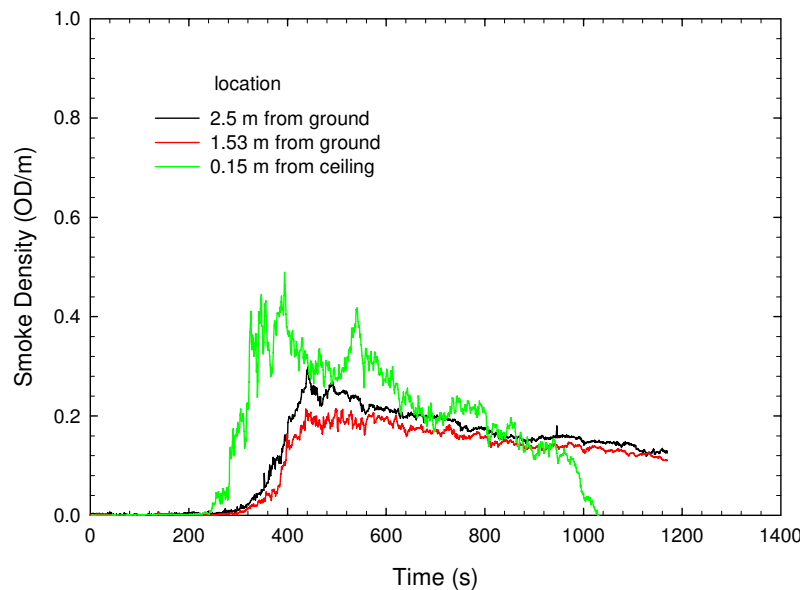


Figure 6.42. Variations of smoke density below the ceiling at center of the tunnel in test T-14 with a passenger compartment fire

As a result, the responses of fire detectors/detection systems to the passenger compartment fire in test T-14 were slow. Two linear heat detection systems D-1L1 and D-2L2 detected the fire at 171 s and 291 s. The optical flame detector D-3F1 had also a slow response to the fire at 173 s. Two visual CCTV detectors D-4C1 and D-6C3 detected the fire at 188 s and 271 s. The smoke detection system D-9S1 responded to the fire at 230 s. Two spot heat detectors D-7H1 and D-8H2 had no response to the fire.

For test T-19 involving polyurethane foam, the foam was sprayed with 100 ml of methyl hydrate and placed behind the simulated passenger compartment. After ignition, the fire grew up quickly. Although the fire size was small, the visible flame and dark smoke generated from the fire could be observed from the front of the passenger compartment, as shown in Figure 6.43. The fire was self-extinguished in 18 minutes after the fuel mass was burnt out.

Smoke densities generated in three stationary vehicle fires, which were measured at 15 cm below the ceiling, were compared in Figure 6.44. Among three fire scenarios, the smoke density generated in the engine compartment fire with gasoline fuel was highest and the smoke density generated in the passenger compartment fire with polyurethane foam grew up earliest.

Due to fire size and type, the linear heat detection system D-1L1 detected the foam fire at 105 s in the test. The optical flame detector D-3F1 responded to the fire at 76 s. The visual CCTV detector D-4C1 detected the fire at 12 s. The smoke detection system D-9S1 responded to the fire at 115 s. Other four detectors and detection systems had no response to the foam fire, as shown in Table 6.2.



Figure 6.43. Polyurethane foam fire in test T-19

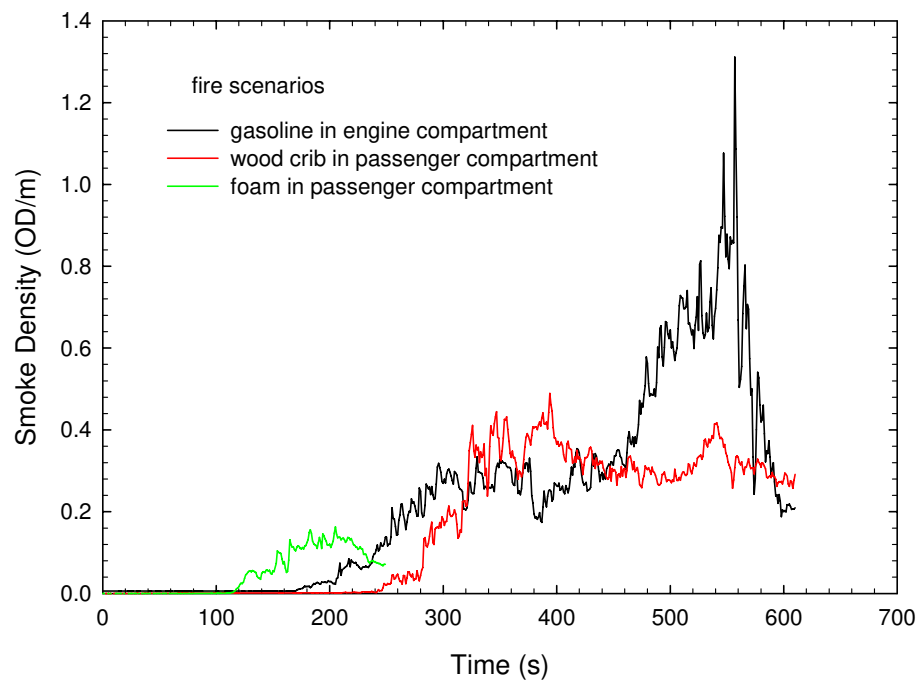


Figure 6.44. Smoke density generated in three simulated stationary vehicle fires measured at 15 cm below the ceiling

6.3. Moving Vehicle Fires

A moving vehicle fire can be caused by many factors, including a fuel delivery failure and ignited by hot exhaust components. The fire is not only a realistic scenario that has occurred on many occasions in tunnels, but it is also a challenge for a fire detection system [1].

A moving fire system was constructed in the test program. The fire source consisted of a fibrefrax pad with a dimension of 0.3 m x 0.3 m, and 50 ml of gasoline was sprayed on the blanket. Its heat release rate was approximately 100 ~ 150 kW, when the fire source was at rest, as shown in Figure 6.45. During tests, the pad was placed and ignited inside a box, preventing the fire from being detected before moving. After ignition, the fire source was dragged by a cable using a high speed winch apparatus at the lane close to south wall of the tunnel. The moving distance of the fire was 30 m from east end to west end of the tunnel. There was no obstacle around the fire source when the fire moved.

Six fire tests with two different driving speeds and driving directions relative to the detectors were conducted. The test conditions and results are listed in Table 6.3.



Figure 6.45. A still fire before it moved in the tunnel

Figure 6.46 shows a moving fire in a speed of 27 km/h facing detectors from east end to west end of the tunnel. The moving fire size was smaller than a still fire and no visible smoke was observed.

For six tests involving different speeds and moving directions, only the optical flame detector D-3F1 detected the moving fire when its speed was 27 km/h ranging from 2 s to 5 s. It had no response when the fire moved at the speed of 50 km/h. Its response time was shorter when it faced the moving fire than that when the fire moved away from the detector. All other detectors/detection systems had no response to this fire scenario as there was no change in temperature and no smoke generation occurred in the tunnel, as shown in Figure 6.47 with a moving fire at speed of 27 km/h.



Figure 6.46. A moving fire at the speed of 27 km/h from east end to west end of the tunnel

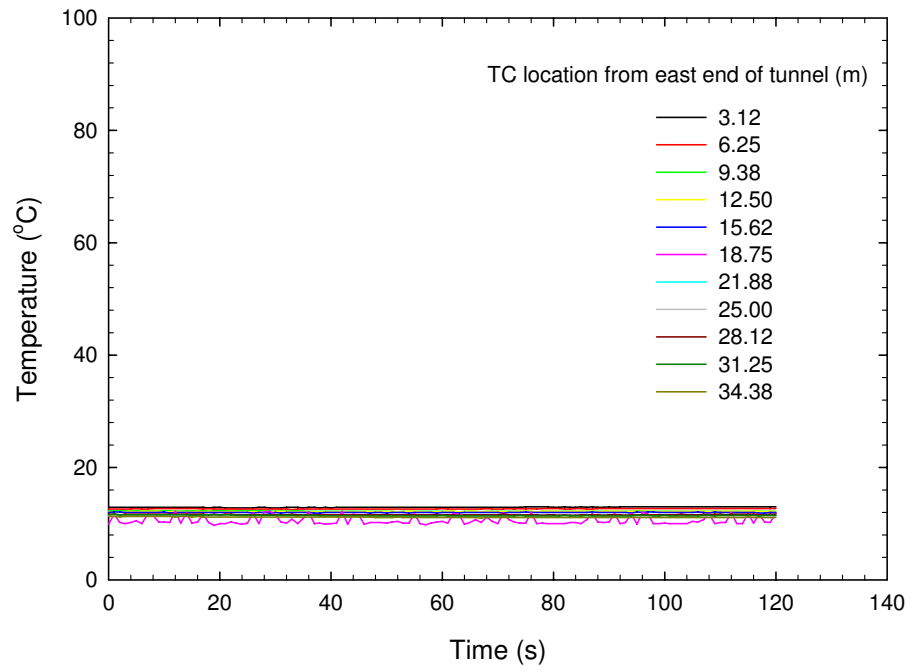


Figure 6.47. Ceiling temperatures along center of the tunnel in Test T-12 with a moving fire at speed of 27 km/h

Table 6.3. Test Conditions and Results in Moving Fire Scenarios

FIRE SCENARIO	TEST NO	FIRE SOURCE	FUEL TYPE	HEAT RELEASE RATE (KW)	T_{ROOM} (°C)	D-1L1 (S)	D-2L2 (S)	D-3F1 (S)	D-4C1 (S)	D-5C2* (S)	D-6C3 (S)	D-7H1 (S)	D-8H2 (S)	D-9S1 (S)
Moving vehicle fire	T-4A	50 km/h, facing	Gasoline	100~150	1	N/A	N/A	N/A	N/A	N/A	N/A	N/A	N/A	N/A
	T-4B	50 km/h, facing	Gasoline	100~150	1	N/A	N/A	N/A	N/A	N/A	N/A	N/A	N/A	N/A
	T-6	50 km/h, away	Gasoline	100~150	1	N/A	N/A	N/A	N/A	N/A	N/A	N/A	N/A	N/A
	T-12	27 km/h, facing	Gasoline	100~150	10	N/A	N/A	2	N/A	N/A	N/A	N/A	N/A	N/A
	T-13A	27 km/h, away	Gasoline	100~150	10	N/A	N/A	4	N/A	N/A	N/A	N/A	N/A	N/A
	T-13B	27 km/h, away	Gasoline	100~150	10	N/A	N/A	4	N/A	N/A	N/A	N/A	N/A	N/A

Note:

- a) No testing data from Detecting System D-5C2 were collected by the project data acquisition system, because of technical malfunction of System D-5C2. The test data of System D-5C2 that are listed in Table 7.1 were provided by the system supplier after the tests, which are not verified by the project.
- b) The systems listed in the table are follows:
 - i. D-1L1: Linear fiber optic heat detection system
 - ii. D-2L2: Linear cable heat detection system
 - iii. D-3F1: Flame detector
 - iv. D-4C1: CCTV flame/smoke detector
 - v. D-5C2: CCTV flame detector
 - vi. D-6C3: CCTV flame detector
 - vii. D-7H1: Spot heat detector
 - viii. D-8H2: Spot heat detector
 - ix. D-9S1: Smoke detection system

7. SUMMARY

Performance of nine selected fire detectors/detection systems was investigated in a laboratory research tunnel facility with a variety of simulated tunnel fire incidents. Test results revealed the fire characteristics of various tunnel fire scenarios, such as their fire growth rate, temperature development and smoke spread in the tunnel. They also demonstrated that the response capabilities of fire detectors/detection systems to a tunnel fire incident were determined by fire size, location and growth rate, fuel types as well as their detecting mechanisms.

Flammable pool fires in the open space, underneath a simulated vehicle and behind a large simulated vehicle developed very quickly and reached their maximum heat release rate within a short period of time. During tests, the gasoline pool fire size was varied from 125 kW (0.3 m x 0.3 m) to 3,400 kW (1.0 m x 2.0 m), generating maximum ceiling temperatures near the fire source ranging from 13°C to 429°C and smoke density at 15 cm below the ceiling at the center of the tunnel from 0.28 OD/m to 2.2 OD/m. The propane fires generated from a burner provided similar fire incident scenarios as those from gasoline pool fires, but no smoke was generated from the propane fires.

The development of the pool fire underneath the vehicle was affected by the existence of the vehicle body above the fire source. In comparison to an open fire, the fire underneath the vehicle grew up slowly due to limited air supply. Small flames were confined underneath the vehicle, making the fire more difficult to be detected. The pool fire behind a large vehicle was a freely burning fire. The existence of the large vehicle body in front of the fire would not affect the burning process of the fire as well as temperature development and smoke spread in the tunnel. However, it significantly obstructed the visual view to the flames. This was a challenging scenario for those detectors that detected fires mainly based on characteristics of flames generated from the fire.

For the small gasoline pool fire (125 kW) in the open space, the optical flame and CCTV detectors responded quickly to the fire. The smoke detection system detected the fire late. Most of heat detectors/detection systems, such as two spot heat detectors and one linear heat detection system in the test program, had no response to the fire, but one linear fiber optic heat detection system also detected the fire quickly based on the temperature raise rate.

Figure 7.1 shows the detecting times of the fire detectors/detection systems to the gasoline pool fires underneath the vehicle. For the small underneath fire (125 kW), only a CCTV flame and smoke detector and a smoke detection system responded to the fire, based on the smoke signals released from the fire. With an increase in fire size, more detectors/detection systems responded to the fires, and their detecting times also reduced. However, the detectors/detection systems evaluated in the test series still showed substantial difference in detecting time even to a large pool fire underneath the vehicle.

Figure 7.2 shows the detecting times of the fire detectors/detection systems to the gasoline pool fires behind a simulated large vehicle. One CCTV flame detector had no response to the fires behind the vehicle, since its view to the flames was obstructed. In comparison to fires underneath the vehicle, more detectors/detection systems were able to detect small fires behind the vehicle and their detecting times decreased with an increase in fire size. In addition, their difference in the detecting time also tended to become small with an increase in fire size.

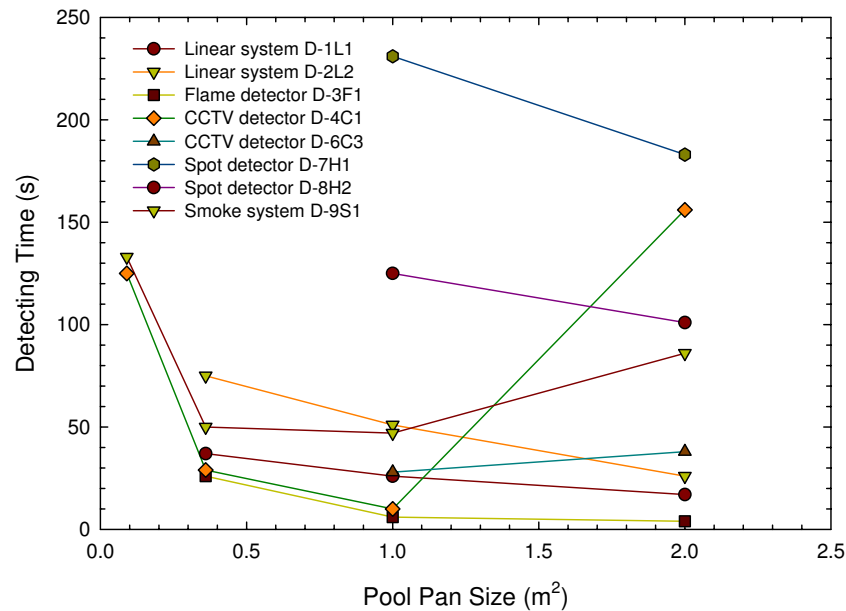


Figure 7.1. Detecting times of fire detectors/detection systems to gasoline pool fire underneath the vehicle

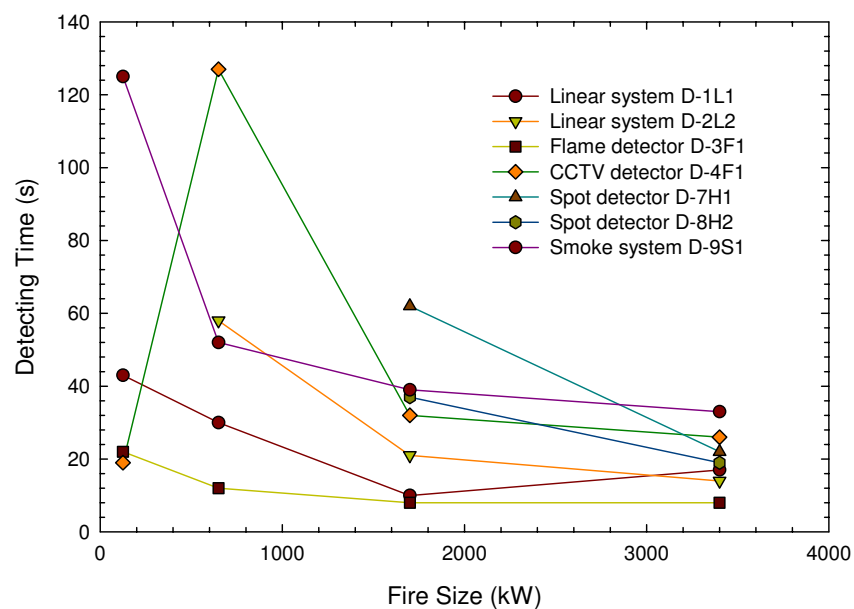


Figure 7.2. Detecting times of fire detectors/detection systems to gasoline pool fire behind the vehicle

Stationary vehicle fires developed much slower than flammable pool fires. During present test series, it took more than 8 minutes for the engine compartment fire involving gasoline, and approximately 6 minutes for the passenger compartment fire involving wood cribs to reach their maximum heat release rates. They generated fires ranging from 1,200 kW to 2,000 kW, maximum ceiling temperatures near the fire source from 95°C to 200°C and smoke density at 15 cm below the ceiling at the center of the tunnel from 0.5 OD/m to 1.0 OD/m. Generally, fire detectors/detection systems had a slow response to the stationary vehicle fires with a slow growth rate.

Figure 7.3 shows the detecting times of fire detectors/detection systems to the fires in the engine and passenger compartment of the stationary vehicle. Except the response of the optical flame detector to the engine compartment fire, the detecting times of fire detectors/detection systems to the simulated stationary vehicle fires were much longer than those to the pool fires. The detecting times to the passenger compartment fire were longer than those to the engine compartment fire, due to difference in fuel type, fire size and location.

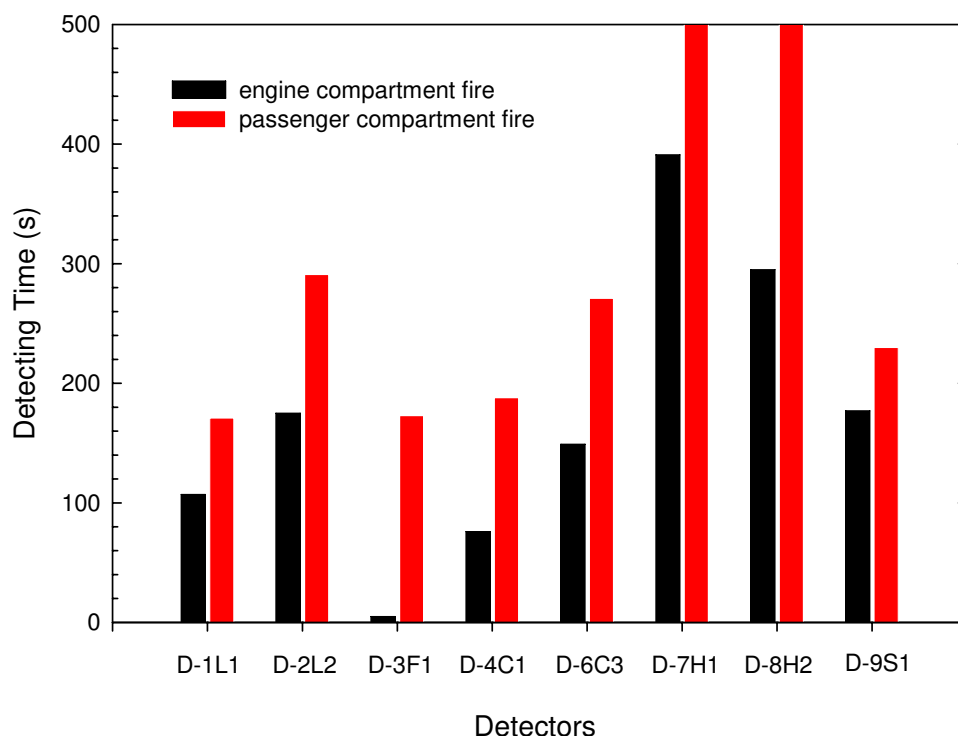


Figure 7.3. Detecting times of fire detectors/detection systems to the simulated stationary vehicle fires

For present test setup, it took a few seconds for a moving fire to pass through the testing tunnel. There was no change in temperature and smoke density in the tunnel when the fire moved fast through the tunnel. Only the optical flame detector detected the moving fire at its speed of 27 km/h, and no other detector/detection system had a response to the moving fire.

Some types of fuels generate a limited amount of smoke or no smoke during a fire incident in the tunnel. The present work showed that such kind of fires, such as propane fires, presented a challenge to those detectors/detection systems that responded to the fire, based on smoke characteristics generated from the fire.

The linear fiber optic heat detection system evaluated in the present work was able to identify the fire location in 2 meters range. Other detector/detection systems were able to identify the fire location within each of their monitoring zone, which range can be changed based on the requirements for fire protection and tunnel geometry.

The visual CCTV fire detectors were able to provide video images to monitor fire conditions in the tunnel. The period of time available for monitoring fire conditions through cameras was reduced with an increase in fire size. For those large fires with a quick growth rate, the period of available time was very short and could be less than 1 minute, as a dark smoker layer was quickly built and descended from the ceiling.

REFERENCES

1. Zalosh, R and Chantranuwat, P., "International Road Tunnel Fire Detection Research Project, Phase 1: Review of Prior Test Programs and Tunnel Fires," The Fire Protection Research Foundation, November 2003.
2. Z. G. Liu, G. P. Crampton, A. H. Kashef, G. D. Loughheed, E. Gibbs, J. Z. Su and N. Benichou, " International Road Tunnel Fire Detection Research Project – Phase II: Task 1, Fire Detectors, Fire Scenarios and Test Protocols," NRCC Client Report (B-4179.1), July 2006
3. G. Crampton, G. Loughheed, "Comparison of Smoke Measurement with Standard and Non-Standard Systems," NRC-IRC Research Report: IRC-RR-183, November 2004
4. J. Mangs and O. Keski-Rahkonen, "Characterization of the Fire Behaviour of a Burning Passenger Car, Part I: Car Fire Experiments," Fire Safety Journal 23 (1994) 17-35
5. J. Mangs and O. Keski-Rahkonen, "Characterization of the Fire Behaviour of a Burning Passenger Car, Part II: Parametrization of Measured Rate of Heat Release Curves," Fire Safety Journal 23 (1994) 37-49
6. A. C. Bwalya, D. Carpenter, M. Kanabus-Kaminska, G. Loughheed, J. Z. Su, B. Taber, N. Benichou, A. Kashef, C. McCartney, A. Bounagui, R. Thomas, "Development of a Fuel Package for Use in Fire Performance of Houses Project," NRC-IRC Research Report: IRC-RR-207, March 2006.